https://ntrs.nasa.gov/search.jsp?R=19930087817 2020-06-17T23:27:55+00:00Z

Restriction/Classification Cancelled

Restriction/Classification Cancelled

391

Copy
RM L53G07a

NACA RM L53G07a

NACA

RESEARCH MEMORANDUM

INVESTIGATION OF SPOILER AILERONS WITH AND WITHOUT A GAP BEHIND THE SPOILER ON A 45° SWEPTBACK WING-FUSELAGE COMBINATION AT MACH NUMBERS FROM 0.60 TO 1.03

By F. E. West, Jr., William Solomon, and Edward M. Brummal

Langley Aeronautical Laboratory
Langley Field, Va.

Restriction/Classification Cancelled

CLASSIFIED DOCUMENT

...e National Defense of the United States within the meaning ... 793 and 794, the transmission or revelation of which in any manner to an unauthorized person is prohibited by law.

CLASSIFICATION CHANGED TO UNCLASSIFIED
AUTHORITY: NACA RESEARCH ABSTRACT NO. 129
EFFECTIVE DATE: JULY 17, 1958
WHL

NATIONAL ADVISORY COMMITTEE
FOR AERONAUTICS

WASHINGTON
September 14, 1953

Restriction/Classification Cancelled

CONFID...

Restriction/Classification Cancelled

NATIONAL ADVISORY COMMITTEE FOR AERONAUTICS

RESEARCH MEMORANDUM

INVESTIGATION OF SPOILER AILERONS WITH AND WITHOUT A GAP BEHIND THE SPOILER ON A 45° SWEPTBACK WING-FUSELAGE COMBINATION AT MACH NUMBERS FROM 0.60 TO 1.03

By F. E. West, Jr., William Solomon, and Edward M. Brummal

SUMMARY

An investigation was conducted with several 73-percent semispan inboard spoiler ailerons, projecting 4 percent of the local wing chord from the wing surface, and located at the 70-percent chord line of a 45° sweptback wing-fuselage combination. The model consisted of a wing with an aspect ratio of 3.98, taper ratio of 0.61, and NACA 65A006 airfoil sections parallel to the plane of symmetry in combination with a blunt-tail fuselage of fineness ratio 10. Six-component force data were obtained during the investigation in the Langley 16-foot transonic tunnel at Mach numbers from 0.60 (Reynolds number of 5.1×10^6) to 1.03 (Reynolds number of 6.2×10^6) for an angle-of-attack range of approximately -2° to 26°.

Although upper-surface-spoiler configurations with a gap in the wing behind the spoiler lost rolling-moment effectiveness above an angle of attack of 6°, they did retain some effectiveness even at high angles of attack for the entire transonic speed range, whereas an upper-surface-spoiler configuration without a gap lost complete effectiveness at high angles of attack for most Mach numbers. The upper-surface-spoiler effectiveness increased with increase in width of the wing gap. Although at low angles of attack the influence of wing-gap width decreased with increase in Mach number, little change in the influence of the gap width occurred at high angles of attack. A lower-surface spoiler was less effective than a corresponding upper-surface spoiler at low angles of attack and produced a substantial rolling moment in the reversed direction at high angles of attack. Two oppositely deflected spoilers were found to be useful mainly in the lower angle-of-attack range where the rolling moment produced was much greater than for a single upper-surface spoiler.

Restriction/Classification Cancelled

INTRODUCTION

Because flap-type ailerons on sweptback wings lose effectiveness with approach to transonic speeds, as indicated in reference 1, the need has existed for a lateral-control device which would retain effectiveness throughout the speed and angle-of-attack range. Spoiler ailerons have been shown to be effective on sweptback wings and their effectiveness has been found to increase through the transonic speed range. (See reference 2.) In addition, spoiler ailerons can be designed with very low hinge moments and they tend to produce less wing twist than conventional flap-type ailerons. Although numerous investigations of spoilers have been conducted at low speeds, most of the spoiler investigations at transonic speeds have been conducted at low angles of attack and low Reynolds numbers. (For example, see ref. 2.) A systematic test program has therefore been initiated in the Langley 16-foot transonic tunnel to obtain force and pressure data for various spoiler configurations in the transonic speed range at moderately high Reynolds numbers and over a wide range of angle of attack. The initial investigation of this program has been conducted on a 45° sweptback wing-fuselage combination at 0° yaw and a Mach number range from 0.60 to 1.03.

The spoilers investigated were of the retractable type and extended along the 70-percent chord line from the fuselage (or 14 percent of the wing semispan) to 87 percent of the wing semispan and were projected from the wing surface 4 percent of the local wing chord. This paper presents the six-component force-test results which were obtained during this initial investigation. Aerodynamic characteristics are shown for an upper-surface-spoiler configuration having various widths of gap in the wing behind the spoiler, for a lower-surface spoiler alone, and for a lower-surface spoiler in combination with an upper-surface spoiler. A comparison is also made between spoiler effectiveness and flap-type aileron effectiveness over the Mach number range.

SYMBOLS

The forces and the moments are presented about the wind axes which have their origin at the intersection of the plane of symmetry and a point which corresponds to the 25-percent-chord station of the mean aerodynamic chord.

b	wing span
c	local wing chord
$\bar{c}$	wing mean aerodynamic chord

C_D	drag coefficient, Drag/qS
C_L	lift coefficient, Lift/qS
C_l	rolling-moment coefficient, Rolling moment/qSb
C_m	pitching-moment coefficient, Pitching moment/qS$\bar{c}$
C_n	yawing-moment coefficient, Yawing moment/qSb
C_Y	lateral-force coefficient, Lateral force/qS
M	free-stream Mach number
P_b	base pressure coefficient, $\frac{p_b - p}{q}$
p_b	static pressure at base of model
p	free-stream static pressure
q	free-stream dynamic pressure
r	fuselage radius
S	total wing area
x	longitudinal distance, positive rearward of fuselage nose.
α	angle of attack of fuselage center line relative to test-section center line
$\Delta C_D, \Delta C_L, \Delta C_m$	incremental coefficients produced by control

APPARATUS

Tunnel.- The investigation reported herein was conducted in the Langley 16-foot transonic tunnel, which is a single-return wind tunnel having a slotted throat of octagonal cross section. The maximum variation of average Mach number was about ±0.002 along the test-section center line in the vicinity of the model. For details of the test-section configuration and of the calibration of the tunnel, see reference 3.

Model.- Figure 1 presents the geometric details of the basic model configuration (model without spoilers) and of the six spoiler configurations tested. The basic model configuration for these tests was a modification of the 45° sweptback wing-fuselage model which was tested previously (ref. 4). The steel wing had NACA 65A006 airfoil sections parallel to the plane of symmetry, quarter-chord-line sweep of 45°, taper ratio of 0.61, and aspect ratio of 3.98. As in the model of reference 4, the wing was designed to have no incidence, dihedral, or twist, and was mounted in a midwing position on the fuselage. The modified fuselage, constructed of steel, with a fineness ratio of 10, had an afterbody which was less tapered than the fuselage of reference 4. For the present tests, the quarter chord of the mean aerodynamic chord was located at the longitudinal position of the maximum fuselage diameter.

The spoilers for these tests (fig. 1) simulated retractable spoiler-aileron configurations pivoted about the 50-percent chord line. Spoilers were tested without a gap in the wing and with gaps of various widths in the wing behind the spoiler. These spoilers were located along the 70-percent chord line and were projected 4 percent of the local wing chord from the wing surface. The spoilers, extended from the fuselage (14 percent of the wing semispan) to the 87-percent wing semispan station and had a sweep angle of 41.6°. The wing gap behind the spoiler, for the configurations with a gap, extended outboard from the 15-percent to the 87-percent wing semispan station. The oppositely deflected spoiler configuration had one spoiler mounted on the upper surface of the left wing and one on the lower surface of the right wing with no gap behind the spoilers.

Base pressures were measured by three orifices located two inches inside the base of the model. The pressures were indicated on a mercury manometer board, which was photorecorded.

Model support system.- A single swept cantilever strut supported the sting-mounted model. This model support has been described in detail in reference 4. The model was near the tunnel center line at all angles of attack. A straight coupling between the sting and the model permitted variations in the angle of attack from -4° to 15°; a 10° coupling extended the range.

TESTS

Forces and moments were measured by a six-component electrical-strain-gage balance mounted within the fuselage. The angle-of-attack range for this investigation was about -2° to 26° at Mach numbers from 0.60 to 0.90. At Mach numbers from 0.94 to 1.03 the maximum angle of attack was limited by allowable sting-support stresses or available

tunnel power. For example, the maximum angle of attack was usually about 12° at a Mach number of 1.03. A few configurations were tested to a Mach number of 1.07 at 0° angle of attack, and a few tests with the basic model were extended to -4° angle of attack. The Reynolds number variation over the speed range of the tests is shown in figure 2.

PRECISION AND CORRECTIONS

Force-data accuracy.- The estimated maximum error of the drag coefficient is ±0.001 at low angles of attack and increases to ±0.005 at the highest angles of attack. The estimated maximum error of the other coefficients is tabulated below:

Lift coefficient	±0.01
Pitching-moment coefficient	±0.005
Rolling-moment coefficient	±0.001
Yawing-moment coefficient	±0.001
Lateral-force coefficient	±0.002

Angle of attack.- The angles of attack presented include an adjustment for an incremental angle, determined from static calibration of model angular deflection as a function of pitching moment and normal-force loads. This incremental angle approaches 2° under some loading conditions. Based on the repeatability of deflection measurements made during the static calibrations, the estimated maximum error of the angle-of-attack measurements is ±0.1°. Tunnel-flow angularity is believed to be small.

Base-pressure adjustments.- Drag and lift data were adjusted to the condition of free-stream static pressure at the model base. The average of the base pressures measured for all the configurations at a given speed and angle of attack, which is shown in figure 3, was used for base-pressure adjustments to the data for all configurations. Maximum scatter from the base-pressure curves was ±0.030, which amounted to a drag coefficient of approximately ±0.0007.

Sting and tunnel-wall effects.- Sting interference was not considered of importance for these tests (other than the effects on the base pressures) because all lateral-control-configuration changes were made on the wing, which was remote from the sting. Although some blockage, lift, and wave-reflection interferences exist in a slotted-wall wind tunnel for a lifting model, the amount and effect of this wall interference is small within the present test Mach number range. (See ref. 5.) Therefore, no corrections for wall interference have been applied to the data presented herein.

RESULTS AND DISCUSSION

Data obtained for the seven configurations tested are presented in plots showing the variation of the aerodynamic characteristics with angle of attack. A comparison of the lift, drag, and pitching-moment characteristics of two upper-surface-spoiler configurations with the basic model characteristics is presented in figure 4. Figures 5, 6 and 7 present the influence of the several spoiler configurations on the rolling-moment, yawing-moment, and lateral-force characteristics as well as on the incremental-lift, drag, and pitching-moment characteristics. In figures 4 to 7, the gap configurations are identified by the gap dimension in the wing surface opposite to that on which the spoiler is mounted, as shown in figure 1.

Effect of Upper-Surface Spoilers on Basic Model Characteristics

Lift coefficient.- Figure 4(a) shows that both upper-surface-spoiler configurations usually produced less lift at a given angle of attack than the basic-model configuration for all Mach numbers. With increases in angle of attack above about 6°, these lift losses decreased.

Drag coefficient.- Figure 4(b) shows for all Mach numbers an appreciable increase in the drag of the spoiler configurations over that of the basic model at low angles of attack. This drag rise decreased rapidly with increasing angle of attack.

Pitching-moment coefficient.- The upper-surface-spoiler configurations produced a positive shift in pitching moment relative to the basic-model trim condition up to approximately 8° angle of attack at the lower Mach numbers (fig. 4(c)). With increase in Mach number, the magnitude of this shift became larger and the shift extended to higher angles of attack. The magnitude of the unstable pitching-moment break occurring at an angle of attack of about 8° tended to be reduced by the upper-surface spoilers. There was generally little influence of the upper-surface spoilers on pitching moment at the highest angles of attack.

Effect of Gap on Spoiler Characteristics

Rolling-moment coefficient.- Figure 5(a) shows that adding a gap through the wing behind an upper-surface spoiler resulted in an increase in rolling-moment effectiveness throughout the transonic speed range for all angles of attack. The beneficial effect of a wing gap at transonic speeds has been previously observed in reference 6. The spoiler

configuration with no wing gap generally became ineffective at an angle of attack of 16°. Although the spoiler configurations with wing gaps experienced a loss of effectiveness above an angle of attack of 6° (fig. 5(a)), they generally, however, did retain a small amount of effectiveness even at the high angles of attack.

The decrease in rolling-moment effectiveness with increase in angle of attack above 6° may not necessarily be accompanied by a proportional decrease in the rate of roll. Reference 7, which presents data up to a Mach number of 0.93, shows that the damping in roll of a 45° sweptback wing configuration decreases at the higher angles of attack. This reduced damping in roll could possibly allow a satisfactory rate of roll even at the low values of rolling-moment coefficient developed by the spoiler configurations at high angles of attack.

Figure 5(a) also shows that the rolling-moment effectiveness of the spoiler configurations increased with increase of the lower-surface gap width throughout the angle-of-attack and Mach number range. Hence, it appears that further increases in the lower-surface gap width would result in increased rolling-moment effectiveness as long as the upper-surface gap remained above some critical width. The influence of the gap width on rolling moment decreased with increase in Mach number at low angles of attack (fig. 5(a)). Little change occurred in the gap effectiveness with increase in Mach number at the high angles of attack.

Study of the results indicated that the one change in upper-surface gap width had no apparent effect on rolling-moment effectiveness. Conjecture as to the reason the lower-surface gap is an important parameter leads to the assumption that this gap acts as a flush air scoop. Such a scoop would tend to have an increased influence as the angle of attack was increased.

Yawing-moment coefficient.- The yawing moment for upper-surface spoilers below an angle of attack of about 12° was found to be either slightly favorable or negligible throughout the test Mach number range (fig. 5(b)). At the higher angles of attack, the upper-surface spoilers tended to produce a slight adverse yawing moment. Gap width had no significant effect below an angle of attack of approximately 12°. Above 12° use of a gap tended to make the yawing moment more adverse than for the spoiler with no gap.

Lateral-force coefficient.- All upper-surface-spoiler configurations tended to produce a positive lateral force at the low and intermediate angles of attack with little effect of gap size, figure 5(c). At angles of attack above approximately 19° a negative lateral force was produced.

Incremental-lift, drag, and pitching-moment coefficients.- The effects of gap width on incremental-lift, incremental-drag and

incremental-pitching-moment coefficients shown in figures 5(d), 5(e), and 5(f), respectively, showed little difference from the effects noted in figure 4 for only two spoiler configurations. In general, the lift loss was greater for the configurations with a wing gap than for the configuration with no wing gap, but there was no apparent trend with gap width. There was negligible effect of gap width on incremental-drag coefficient. Increases in gap width, however, had a tendency to increase the positive pitching-moment increment at the higher angles of attack and Mach numbers.

Comparison of Upper- and Lower-Surface Spoiler Characteristics

Rolling-moment coefficient.- In figure 6(a), it is shown that the lower-surface spoiler with 0.028 chord gap was less effective than the corresponding upper-surface spoiler. The lower-surface spoiler tended to reverse rolling-moment effectiveness between 8° and 10° angle of attack and to produce a substantial rolling moment in the reversed direction at the higher angles of attack.

Other coefficients.- Figure 6(b) shows that the lower-surface spoiler produced an adverse yawing moment over almost the entire Mach number range and angle-of-attack range tested. The magnitude of this adverse yaw near an angle of attack of 0° was approximately equal to that of the favorable yaw produced by the upper-surface spoiler. Lift and pitching-moment increments (figs. 6(d) and (f), respectively) produced by the lower-surface spoiler exhibited a reversal of sign at approximately the same angles of attack at which rolling moment showed reversals of sign. Since the basic model tended to develop a pitch-up starting in the region of 8° to 10° angle of attack (see fig. 4(c)), the reversal of sign of the incremental pitching moment (from negative to positive), figure 6(f), indicates that the pitch-up would be more severe for the configuration with the lower-surface spoiler than for the basic model. At moderate angles of attack the drag increment produced by the lower-surface spoiler (fig. 6(c)) was larger than that produced by the upper-surface spoiler.

Comparison of Upper-Surface Spoiler With Oppositely Deflected Spoilers

Rolling-moment coefficient.- The oppositely deflected spoilers, figure 7(a), produced greater rolling moments than a single upper-surface spoiler up to angles of attack of approximately 10° at which angle it was noted in the discussion of figure 6(a) that a lower-surface spoiler tended to reverse effectiveness. (No gap was used in the wing for the

oppositely deflected and the upper-surface spoilers discussed herein.) At the higher angles of attack the oppositely deflected spoiler configuration tended to reverse effectiveness as would be expected since figure 6(a) indicates that a lower-surface spoiler produced a substantial rolling moment in the reversed direction. This oppositely deflected spoiler configuration would, therefore, be useful only in the lower angle-of-attack range.

Other coefficients.- The variation of yawing-moment, lateral-force, incremental-lift, incremental-drag, and incremental-pitching-moment coefficient with an angle of attack (figs. 7(b), (c), (d), (e), and (f), respectively) for the oppositely deflected spoilers could have been predicted approximately from the corresponding curves for the upper- and for the lower-surface spoilers shown in figures 6(b) to 6(f). For instance, the negligible yawing moments for the oppositely deflected spoilers up to an angle of attack of 4° would be expected from the equal and opposite yawing moments noted in figure 6(b) at the low angles of attack.

The failure of the incremental lift curve for the oppositely deflected spoilers to show no lift at an angle of attack of 0°, (fig. 7(d)), is believed to be caused mainly by a difference in spoiler mounting (fig. 1), which may have allowed some small model aerodynamic asymmetry to exist.

Effect of Mach Number on Spoiler Effectiveness

The variation of the rolling-moment coefficient with Mach number of several spoiler configurations is shown in figure 8. Trends with Mach number shown for the upper-surface spoiler configuration with 0.028-chord wing gap are representative of all the upper-surface spoiler configurations tested, although the magnitude of the rolling-moment coefficient may differ.

At 0° and 4° angle of attack there was a gradual increase with Mach number in the upper-surface, the lower-surface, and consequently in the oppositely deflected spoiler effectiveness that approached a maximum at a Mach number of 0.94 and then decreased slightly with further increase in Mach number. At an angle of attack of 8° the lower-surface spoiler lost effectiveness with increase in Mach number; at an angle of attack of 12° and above, the lower-surface spoiler produced a reversed rolling moment at all Mach numbers. Both these effects tended to nullify the rolling-moment effectiveness of the oppositely deflected spoiler configuration at the higher angles of attack. Only the upper-surface spoiler with 0.028-chord wing gap retained some effectiveness over the transonic Mach number range even at the high angles of attack. As noted in the discussion of figure 5(a), this upper-surface spoiler with 0.028-chord gap had the greatest effectiveness of any of the upper-surface spoilers with a gap.

Comparison of Spoiler Effectiveness With Aileron Effectiveness

As a means of illustrating the relative effectiveness of the best spoiler configuration reported herein, figure 9 presents the approximate deflection (obtained by extrapolation of the data of ref. 1) of 30-percent-chord flap-type ailerons required to produce the same rolling moment as the upper-surface spoiler with 0.028-chord wing gap. No evaluation has been made of rolling-moment requirements desired for flight conditions. These deflections are for ailerons located on only one wing semispan and were obtained on a reflection-plane model that is smaller, but almost geometrically similar to the model described in this paper (ref. 1). The 0.43-semispan and the 0.86-semispan ailerons extended from the fuselage to 57 percent and 100 percent of the wing semispan, respectively. An increase in aileron deflection with increase in Mach number is required for both the aileron configurations. The 0.43-semispan inboard aileron, in fact, requires an excessive deflection angle at the higher Mach numbers.

CONCLUSIONS

An investigation was conducted with several 73-percent semispan inboard spoiler ailerons having a height of 4 percent of the local wing chord and located along the 70-percent chord line of a 45° sweptback wing-fuselage combination. Six-component force data were obtained at Mach numbers from 0.60 (Reynolds number, 5.1×10^6) to 1.03 (Reynolds number, 6.2×10^6) for an angle-of-attack range that usually extended from -2° to 20° or higher. The results of the investigation indicate the following conclusions:

1. Upper-surface-spoiler configurations with a gap in the wing behind the spoiler lose rolling-moment effectiveness above an angle of attack of 6° but they do retain some effectiveness even at high angles of attack for the entire transonic speed range, whereas the same type of spoiler configuration without a gap loses complete effectiveness at high angles of attack for most Mach numbers.

2. Rolling-moment effectiveness of the upper-surface-spoiler configurations increases as the lower-surface wing-gap width is increased. At low angles of attack the influence of lower-surface wing-gap width on the rolling-moment effectiveness of the upper-surface-spoiler configurations decreases with increase in Mach number. At high angles of attack, however, little change occurs in the influence of the lower-surface gap width on the effectiveness with increase in Mach number.

3. The lower-surface spoiler with 0.028-chord wing gap is less effective at low angles of attack than the corresponding upper-surface spoiler. This lower-surface spoiler reverses effectiveness between angles of attack of 8° and 10° and produces a substantial rolling moment in the reversed direction at high angles of attack.

4. For two oppositely deflected spoilers, the rolling-moment effectiveness at low angles of attack is much greater than for the single upper-surface spoiler, but reversal of effectiveness occurs at angles of attack above approximately 12°, where the reversed effectiveness of the lower-surface spoiler becomes predominant.

Langley Aeronautical Laboratory,
National Advisory Committee for Aeronautics,
Langley Field, Va., July 2, 1953.

REFERENCES

1. Vogler, Raymond D.: Lateral-Control Investigation of Flap-Type Controls on a Wing With Quarter-Chord Line Swept Back 45°, Aspect Ratio 4, Taper Ratio 0.6, and NACA 65A006 Airfoil Section. Transonic Bump Method. NACA RM L9F29a, 1949.

2. Hammond, Alexander D.: Lateral-Control Investigation of Flap-Type and Spoiler-Type Controls on a Wing with Quarter-Chord-Line Sweepback of 60°, Aspect Ratio 2, Taper Ratio 0.6, and NACA 65A006 Airfoil Section. Transonic Bump Method. NACA RM L50E09, 1950.

3. Ward, Vernon G., Whitcomb, Charles F., and Pearson, Merwin D.: Air-Flow and Power Characteristics of the Langley 16-Foot Transonic Tunnel with Slotted Test Section. NACA RM L52E01, 1952.

4. Hallissy, Joseph M., and Bowman, Donald R.: Transonic Characteristics of a 45° Sweptback Wing-Fuselage Combination. Effect of Longitudinal Wing Position and Division of Wing and Fuselage Forces and Moments. NACA RM L52K04, 1953.

5. Whitcomb, Charles F., and Osborne, Robert S.: An Experimental Investigation of Boundary Interference on Force and Moment Characteristics of Lifting Models in the Langley 16- and 8-Foot Transonic Tunnels. NACA RM L52L29, 1953.

6. Hammond, Alexander D. and Watson, James M.: Lateral-Control Investigation at Transonic Speeds of Retractable Spoiler and Plug-Type Spoiler-Slot Ailerons on a Tapered 60° Sweptback Wing of Aspect Ratio 2. NACA RM L52F16, 1952.

7. Kuhn, Richard E.: Notes on Damping in Roll and Load Distributions in Roll at High Angles of Attack and High Subsonic Speed. NACA RM L53G13a, 1953.

Fuselage coordinates							
x	r	x	r	x	r	x	r
0.000	0.000	9.000	1.936	42.000	4.719	78.000	4.580
0.600	0.227	12.000	2.365	48.000	4.876	84.000	4.245
0.900	0.358	18.000	3.112	54.000	4.971	90.000	3.853
1.500	0.514	24.000	3.708	60.000	5.000	96.000	3.420
3.000	0.866	30.000	4.158	66.000	4.955	100.000	3.125
6.000	1.446	36.000	4.489	72.000	4.830		

Wing data	
Taper ratio	0.61
Aspect ratio	3.98
Wing area	9.04 sq. ft.
Airfoil section	NACA 65A-006 (Parallel to plane of symmetry)

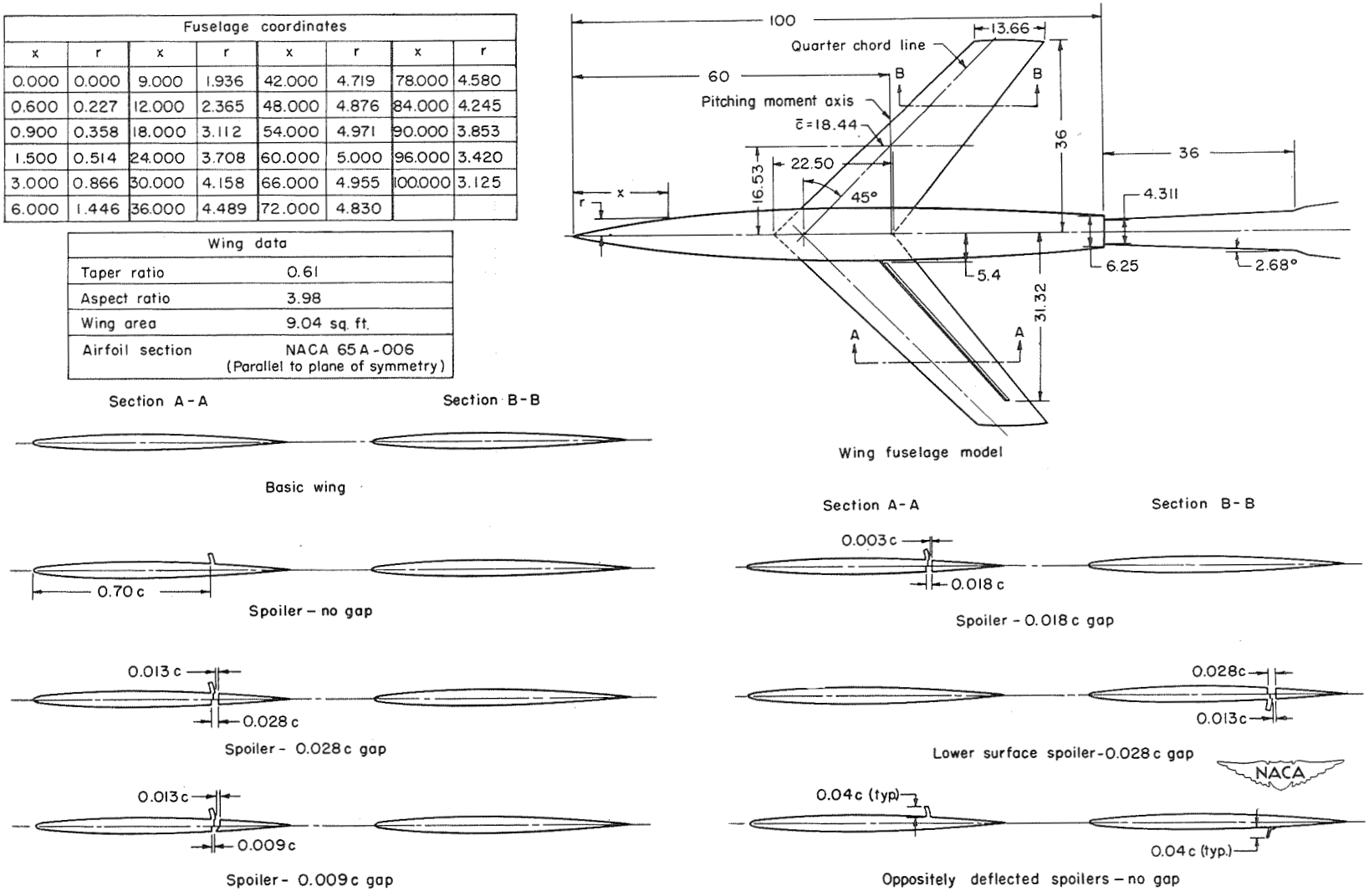

Figure 1.- Diagram of the wing-fuselage model and dimensional details of the several spoiler configurations. (All linear dimensions in inches.)

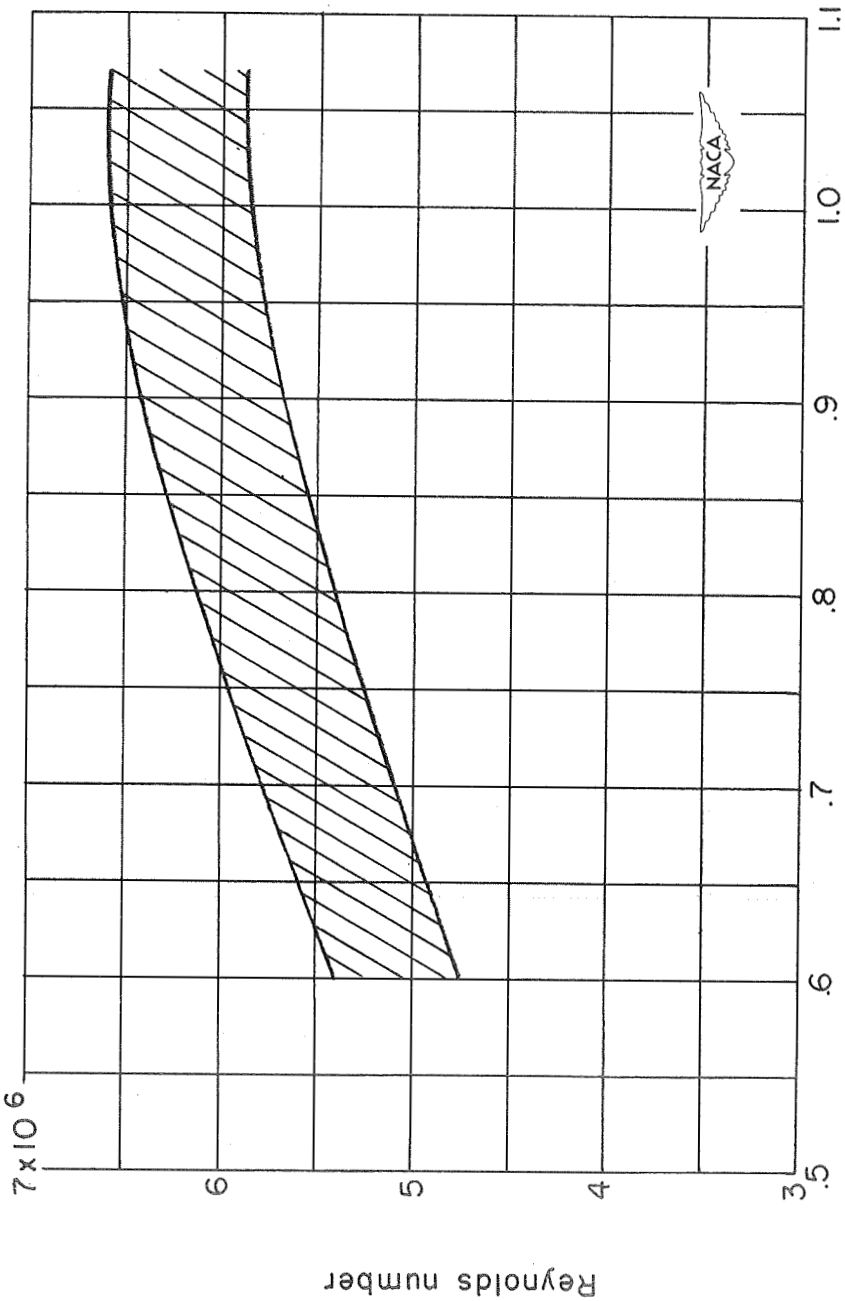

Figure 2.- Variation of Reynolds number (based on mean aerodynamic chord) with Mach number.

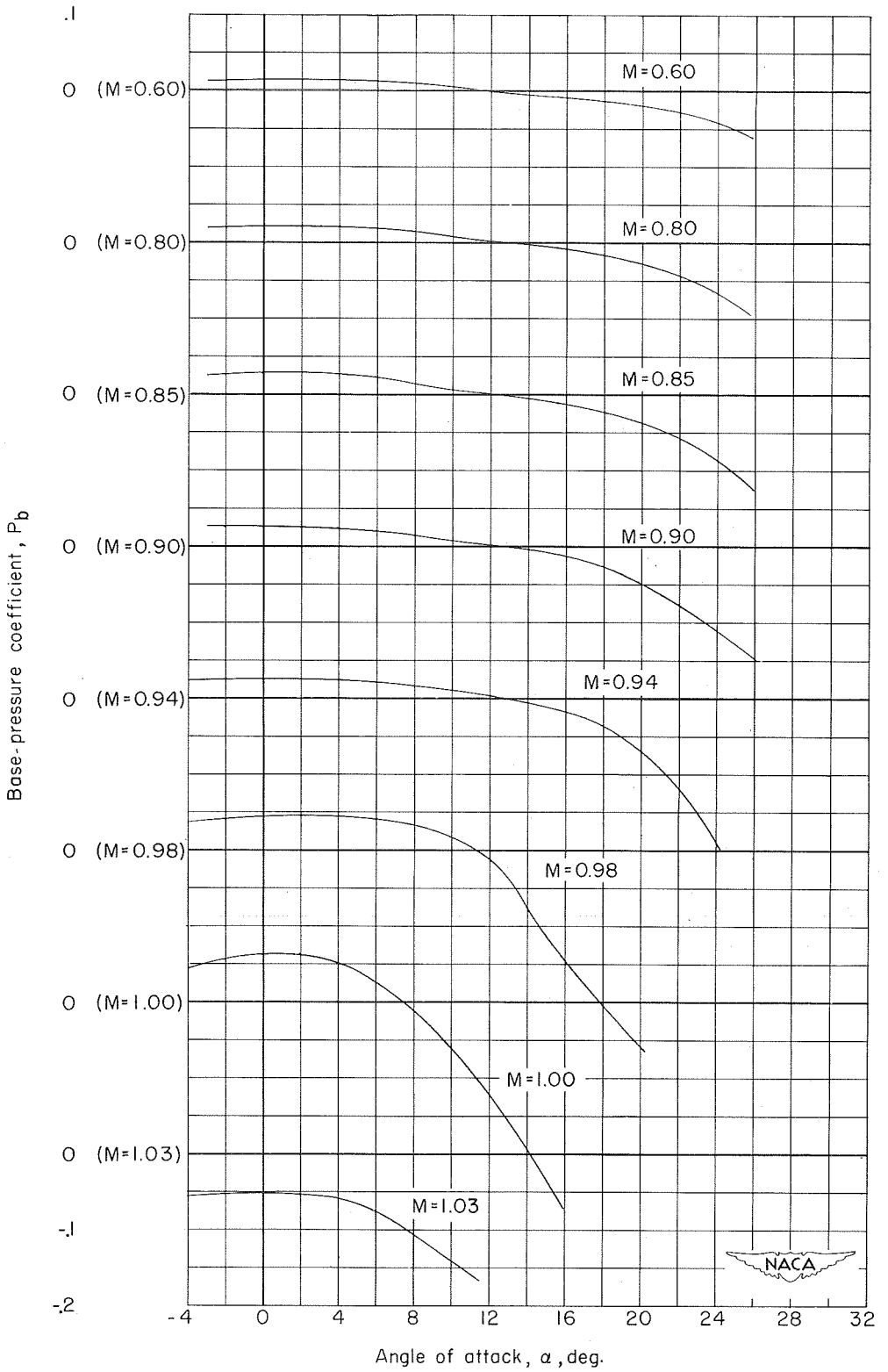

Figure 3.- Average base-pressure coefficient for all configurations.

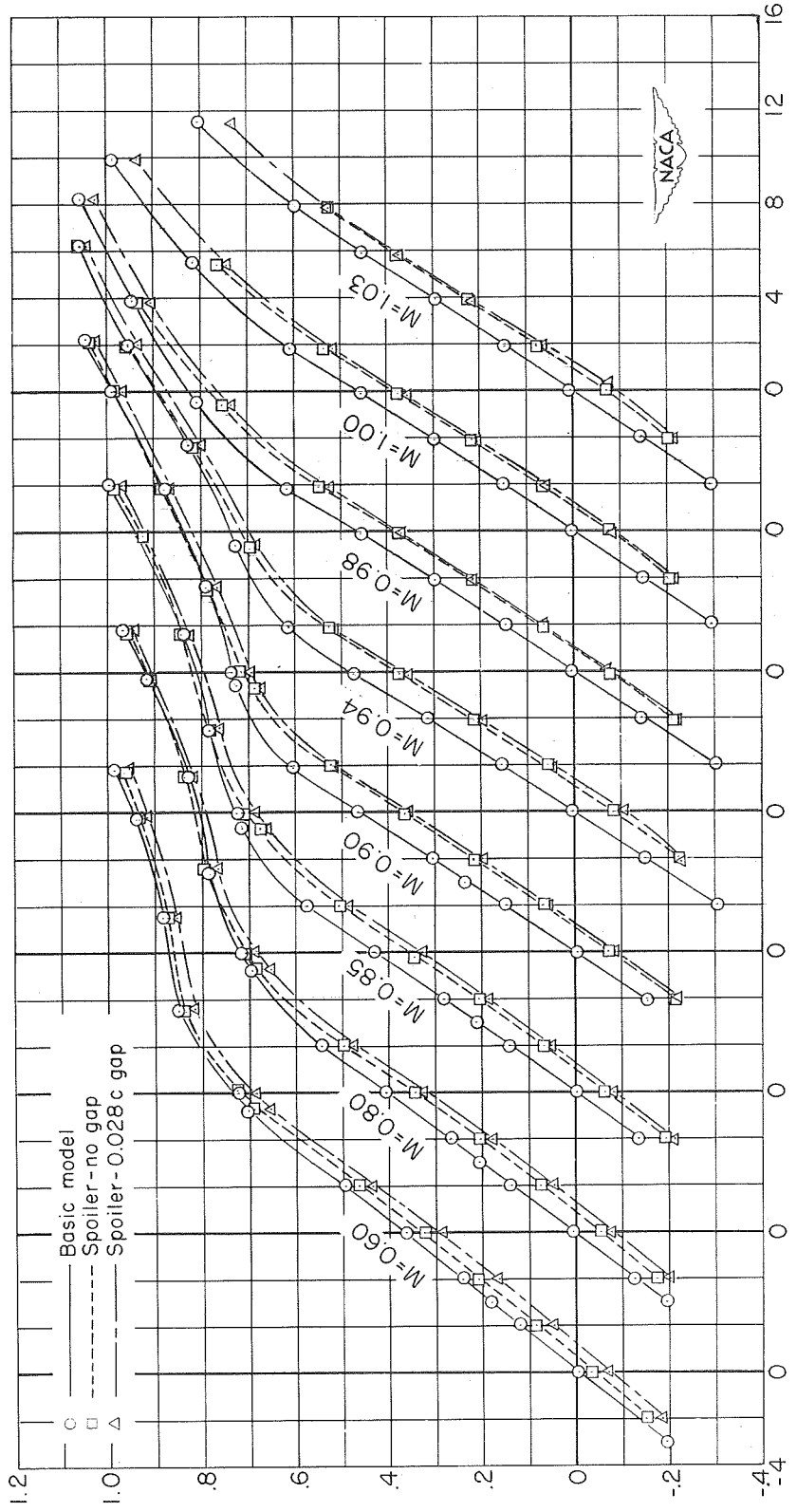

(a) Lift coefficient.

Figure 4.- Comparison of the lift, drag, and pitching-moment characteristics for two upper-surface spoiler configurations with the characteristics for the basic model. Spoilers on left wing.

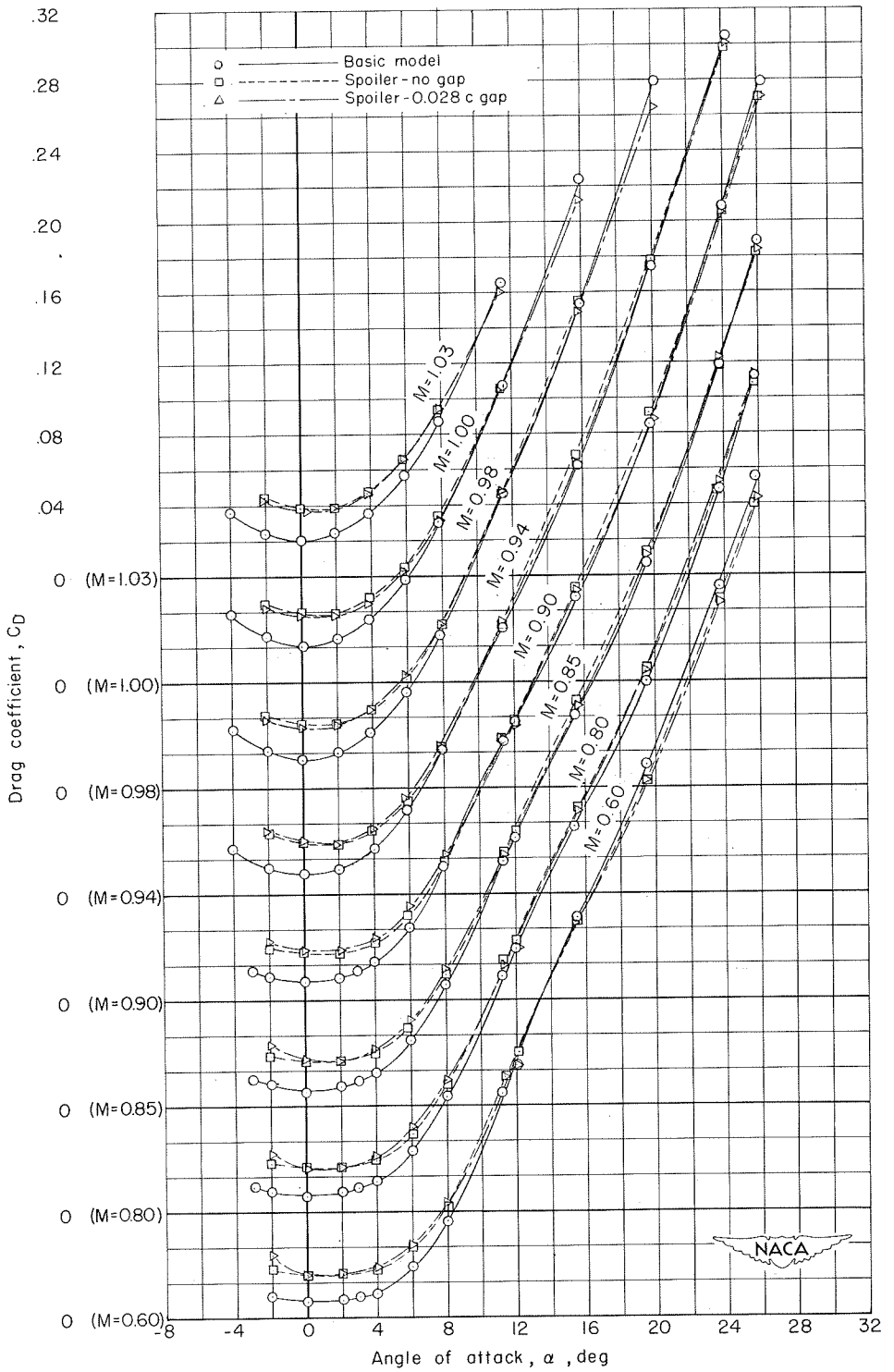

(b) Drag coefficient.

Figure 4.- Continued.

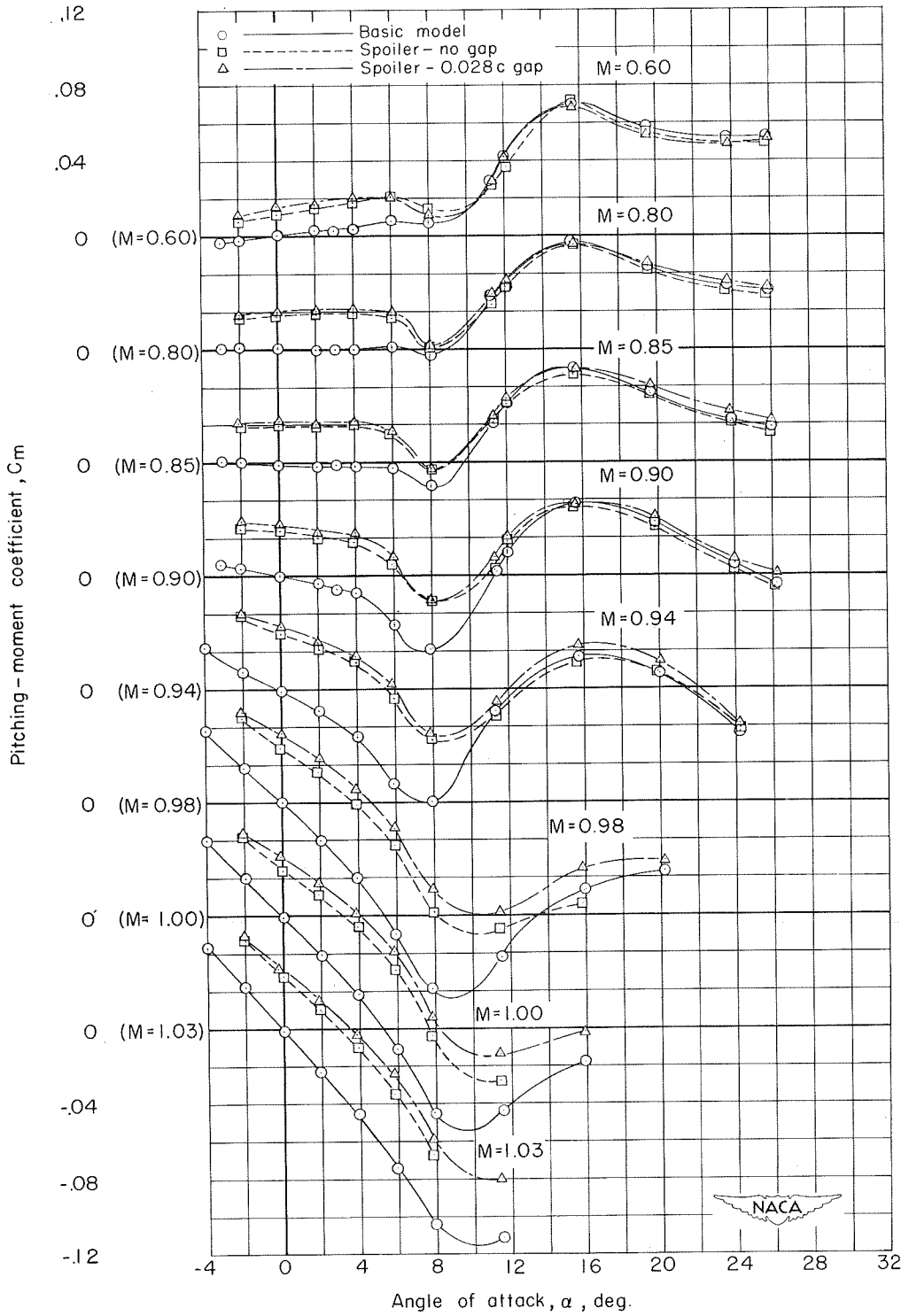

(c) Pitching-moment coefficient.

Figure 4.- Concluded.

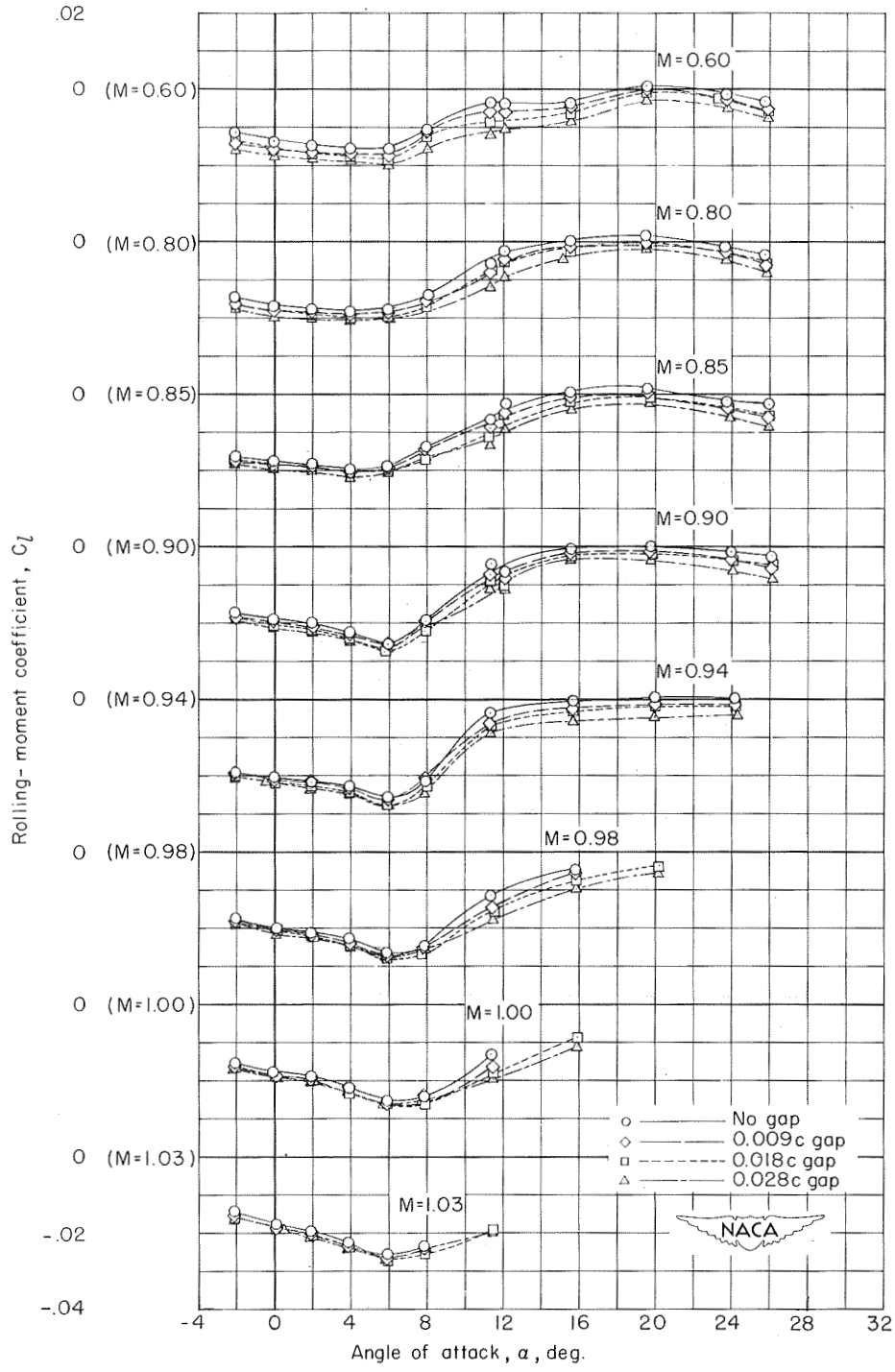

(a) Rolling-moment coefficient.

Figure 5.- Comparison of the aerodynamic characteristics of several upper-surface spoiler configurations showing the effect of variations in the width of the wing gap behind the spoilers. Spoilers on left wing.

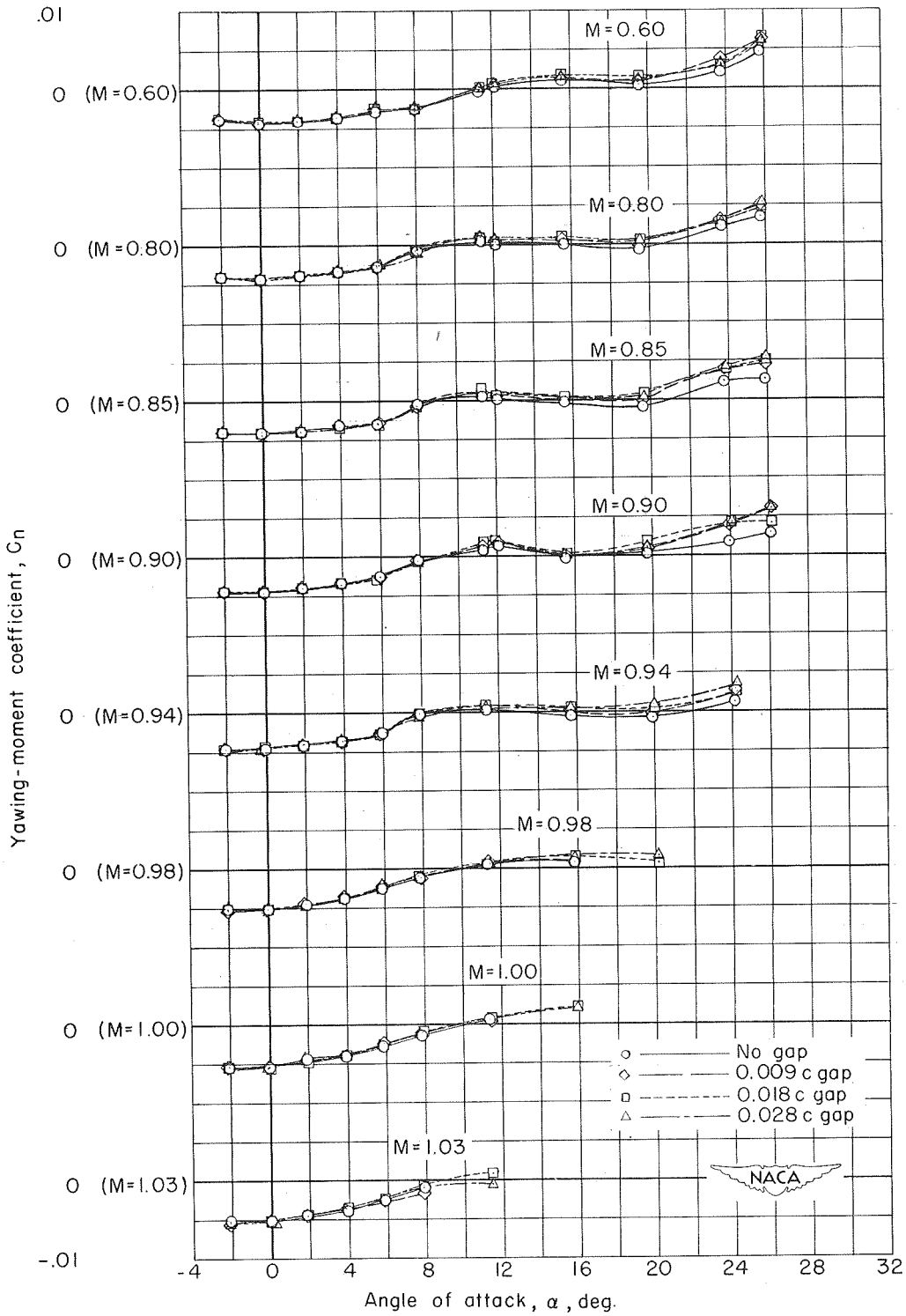

(b) Yawing-moment coefficient.

Figure 5.- Continued.

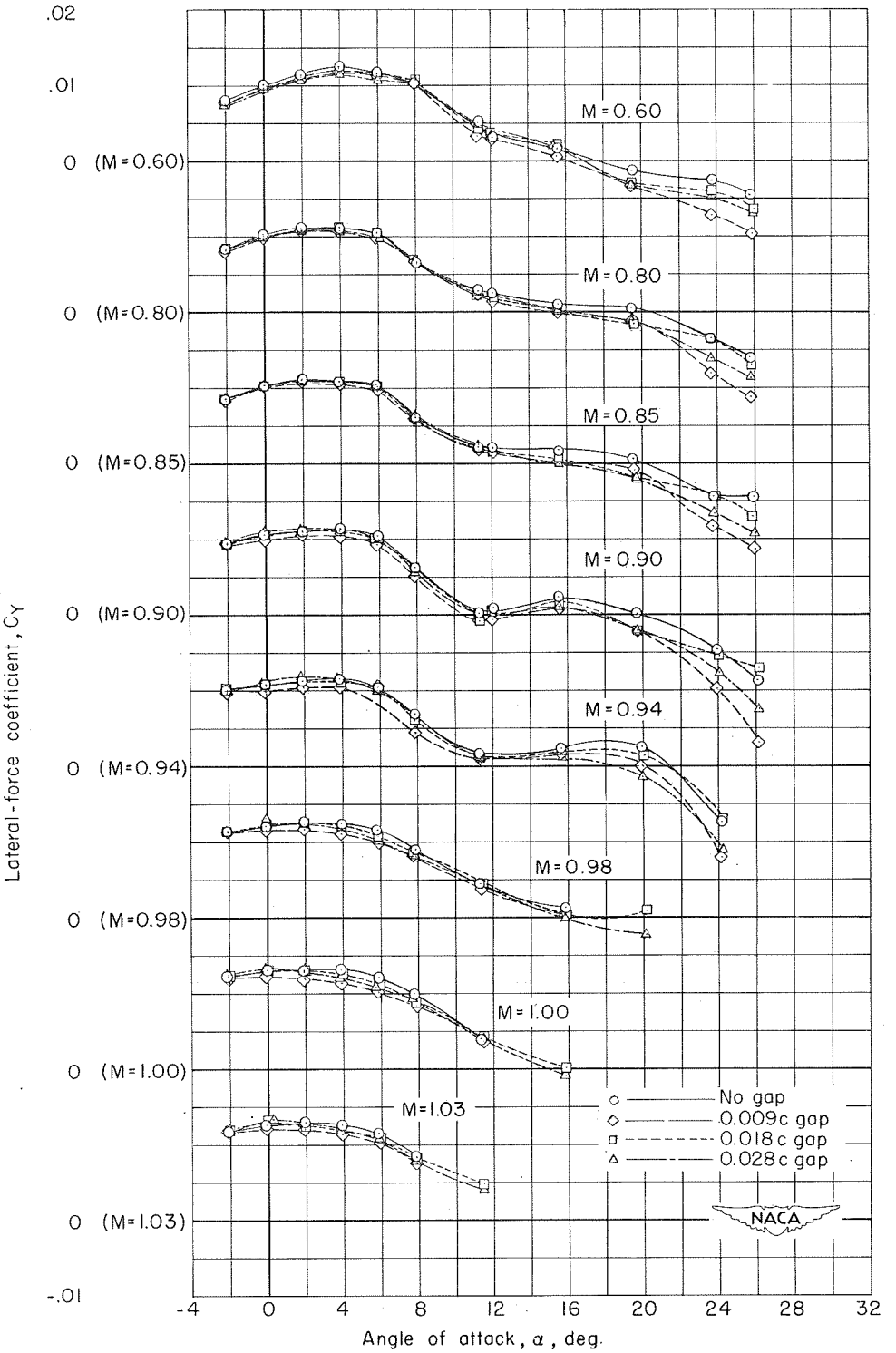

(c) Side-force coefficient.

Figure 5.- Continued.

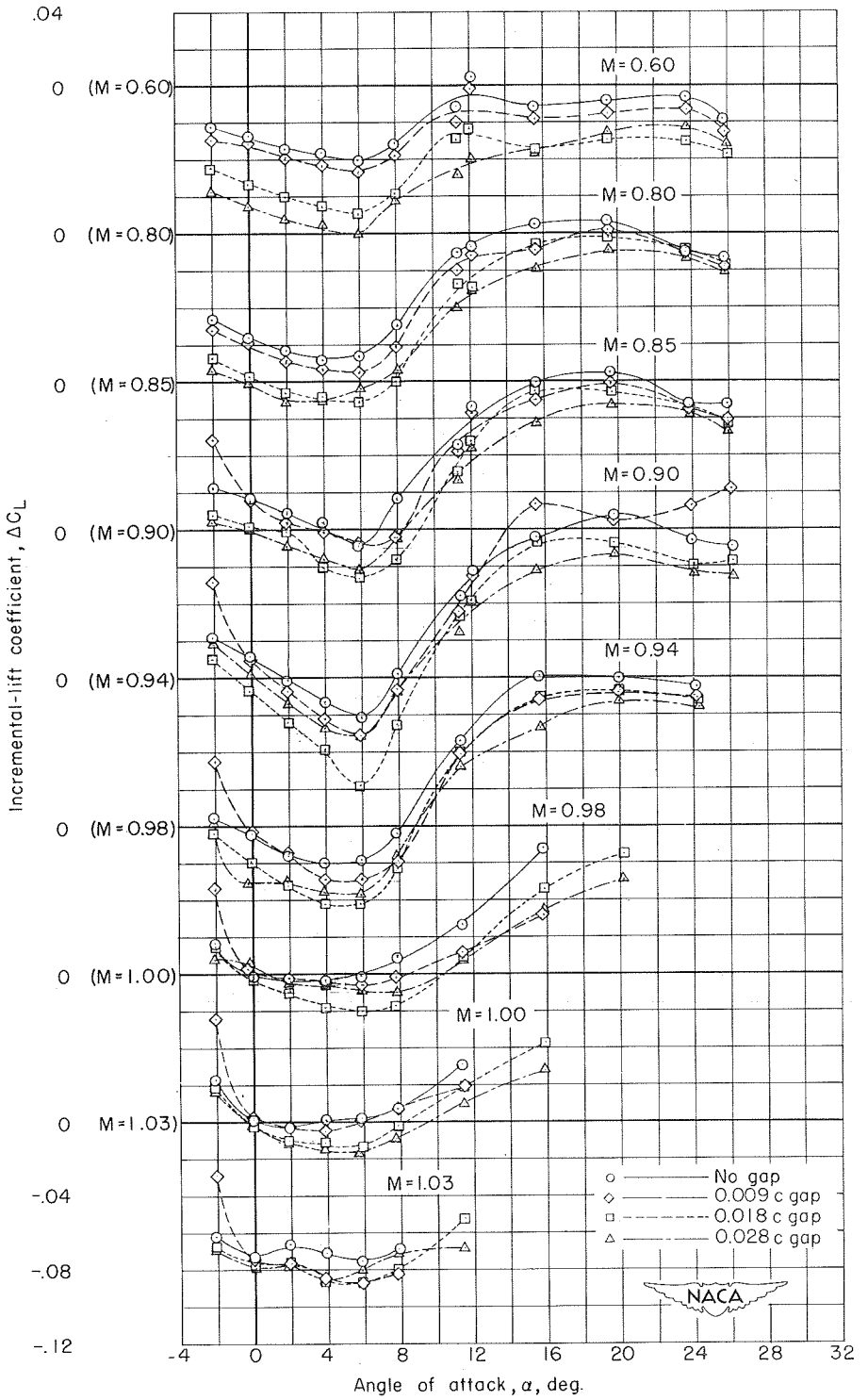

(d) Incremental-lift coefficient.

Figure 5.- Continued.

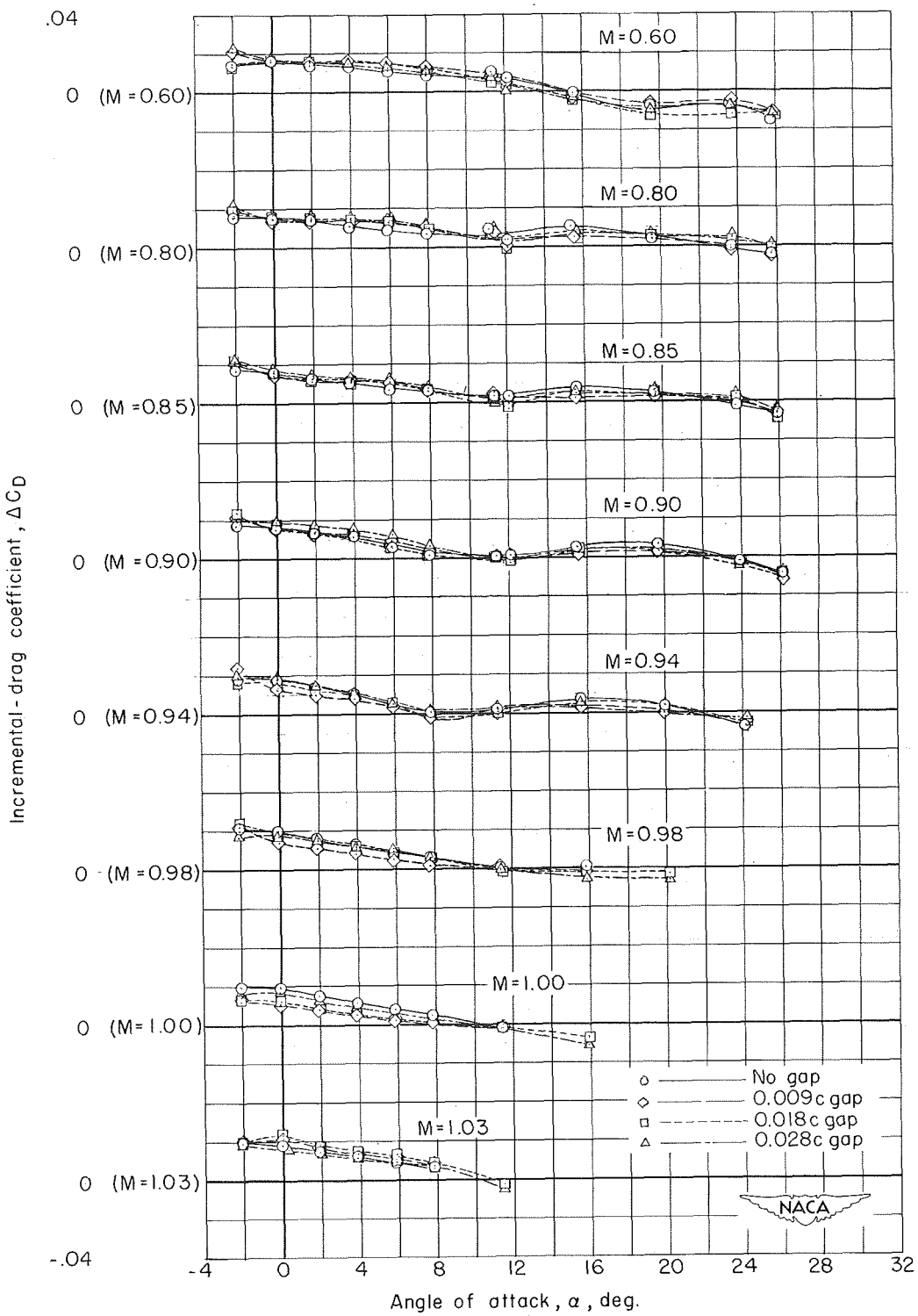

(e) Incremental-drag coefficient.

Figure 5.- Continued.

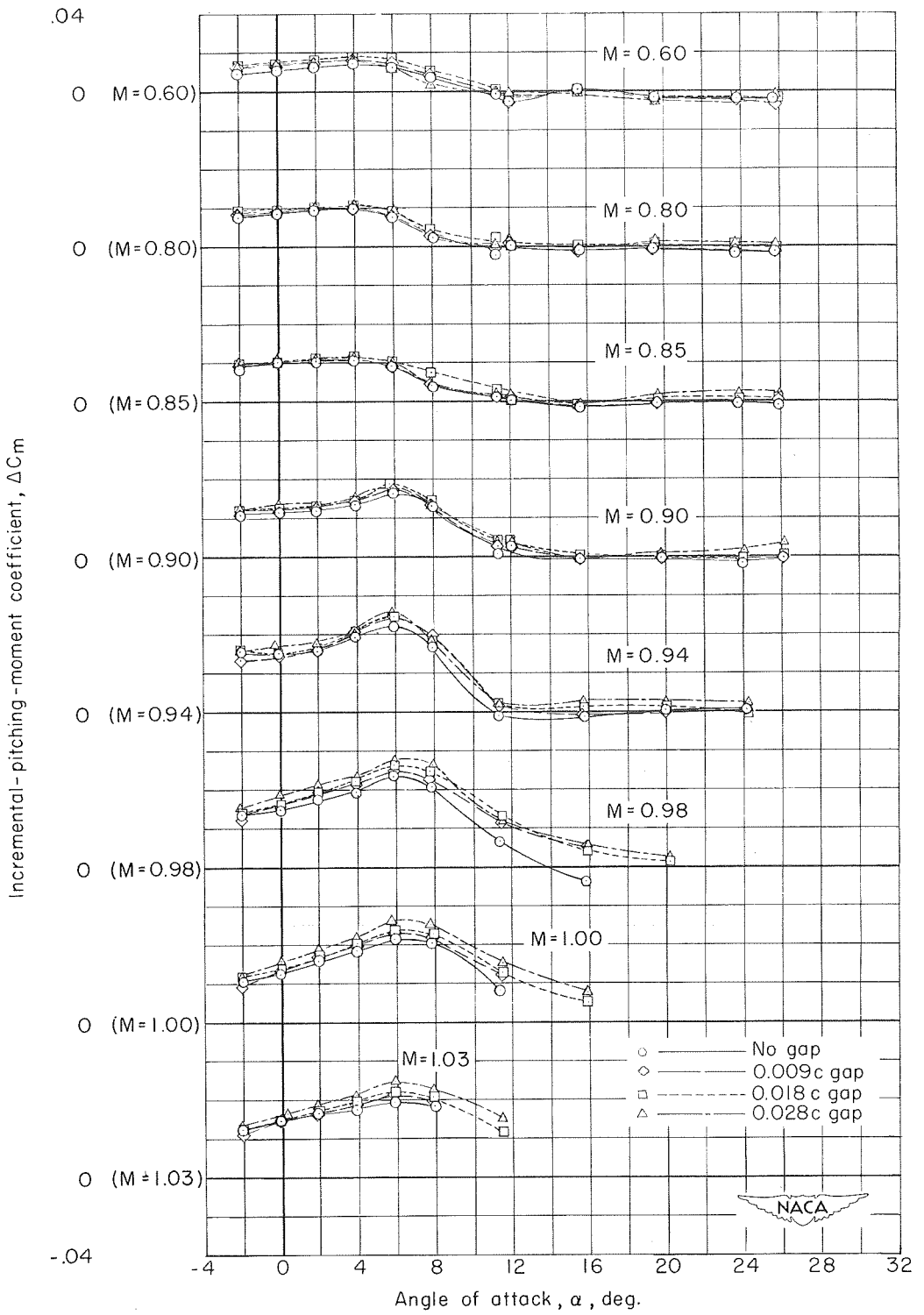

(f) Incremental-pitching-moment coefficient.

Figure 5.- Concluded.

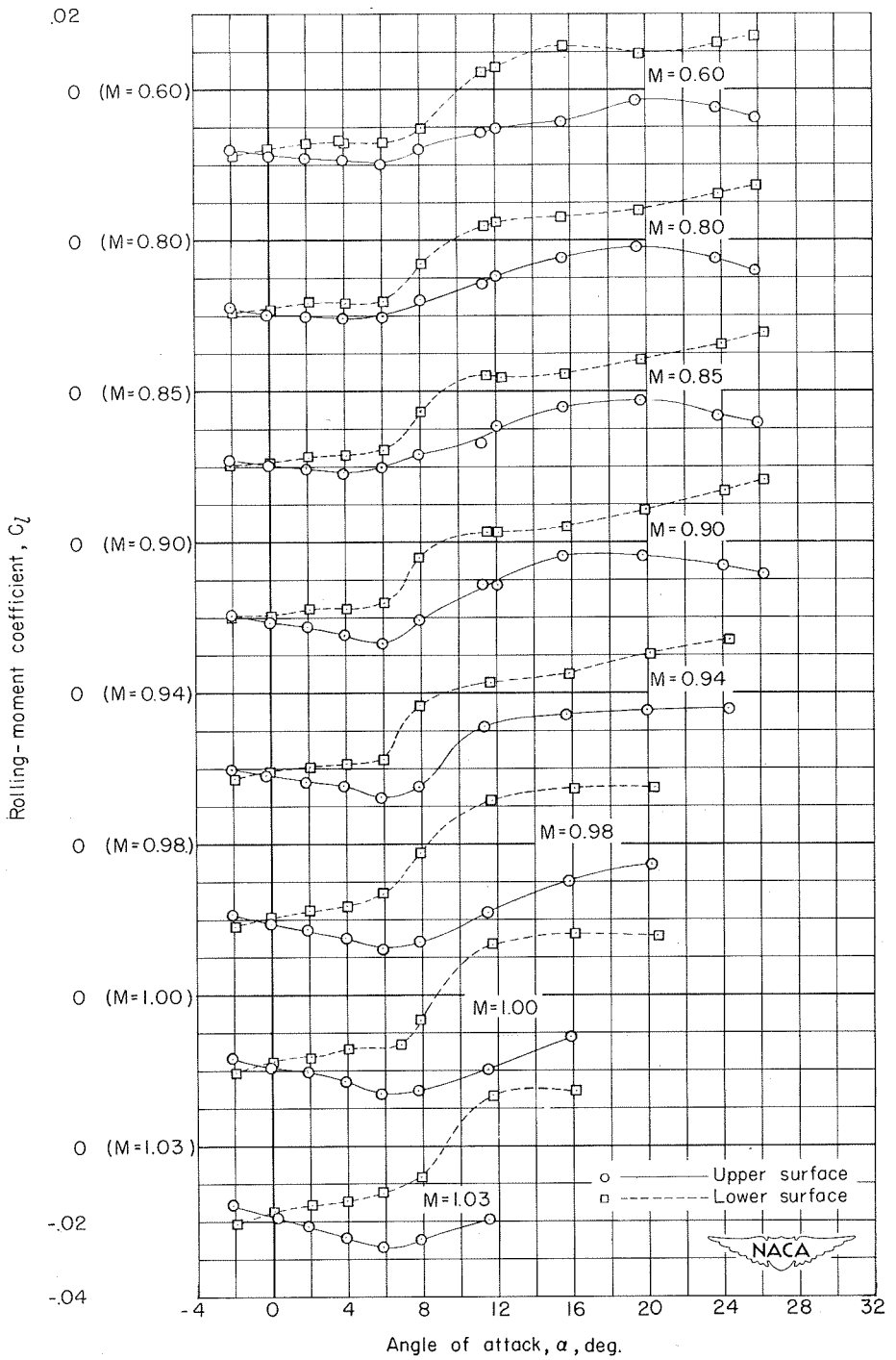

(a) Rolling-moment coefficient.

Figure 6.- Comparison of the aerodynamic characteristics of an upper-surface spoiler on left wing with a lower-surface spoiler on right wing. 0.028c wing gap.

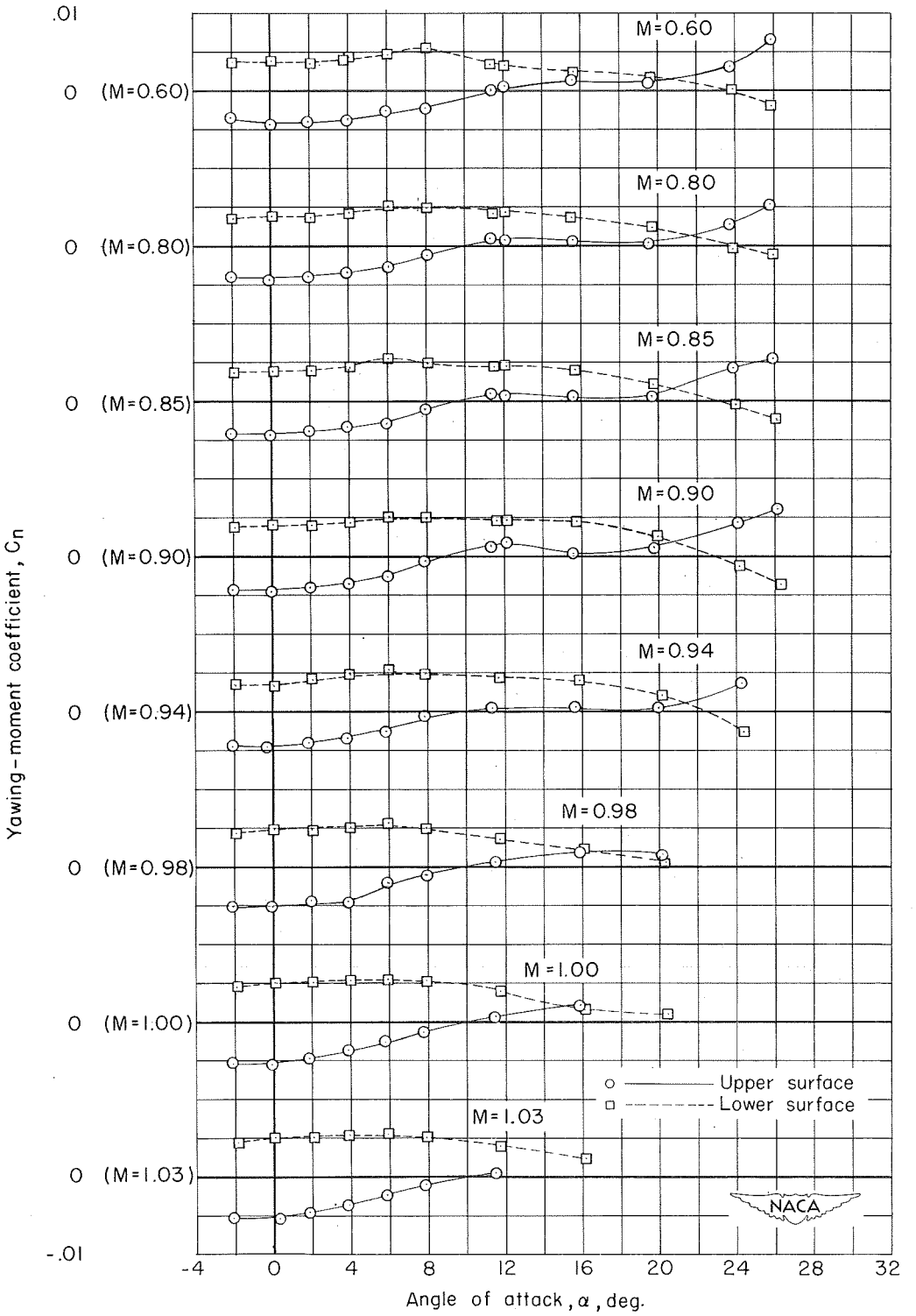

(b) Yawing-moment coefficient.

Figure 6.- Continued.

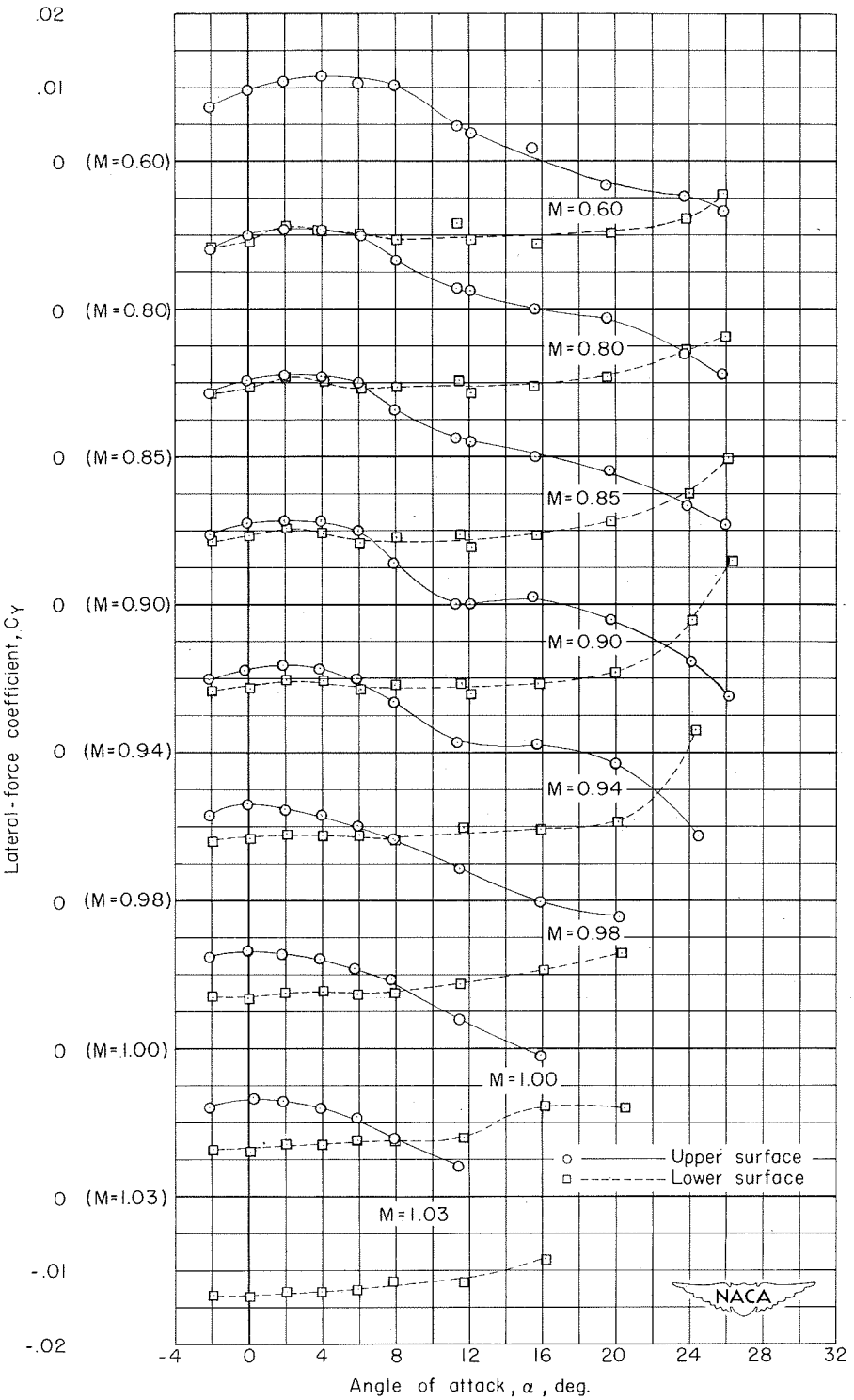

(c) Side-force coefficient.

Figure 6.- Continued.

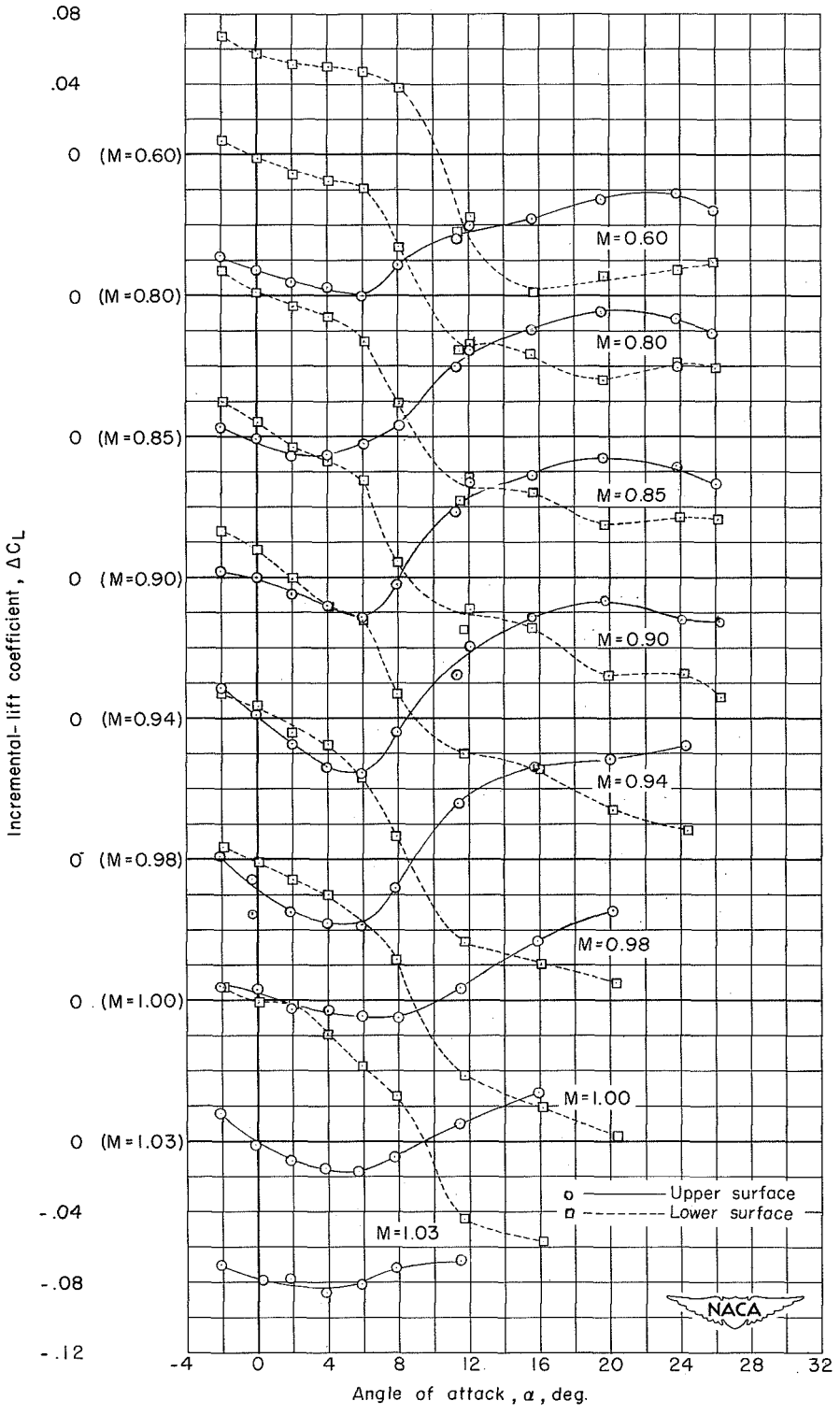

(d) Incremental-lift coefficient.

Figure 6.- Continued.

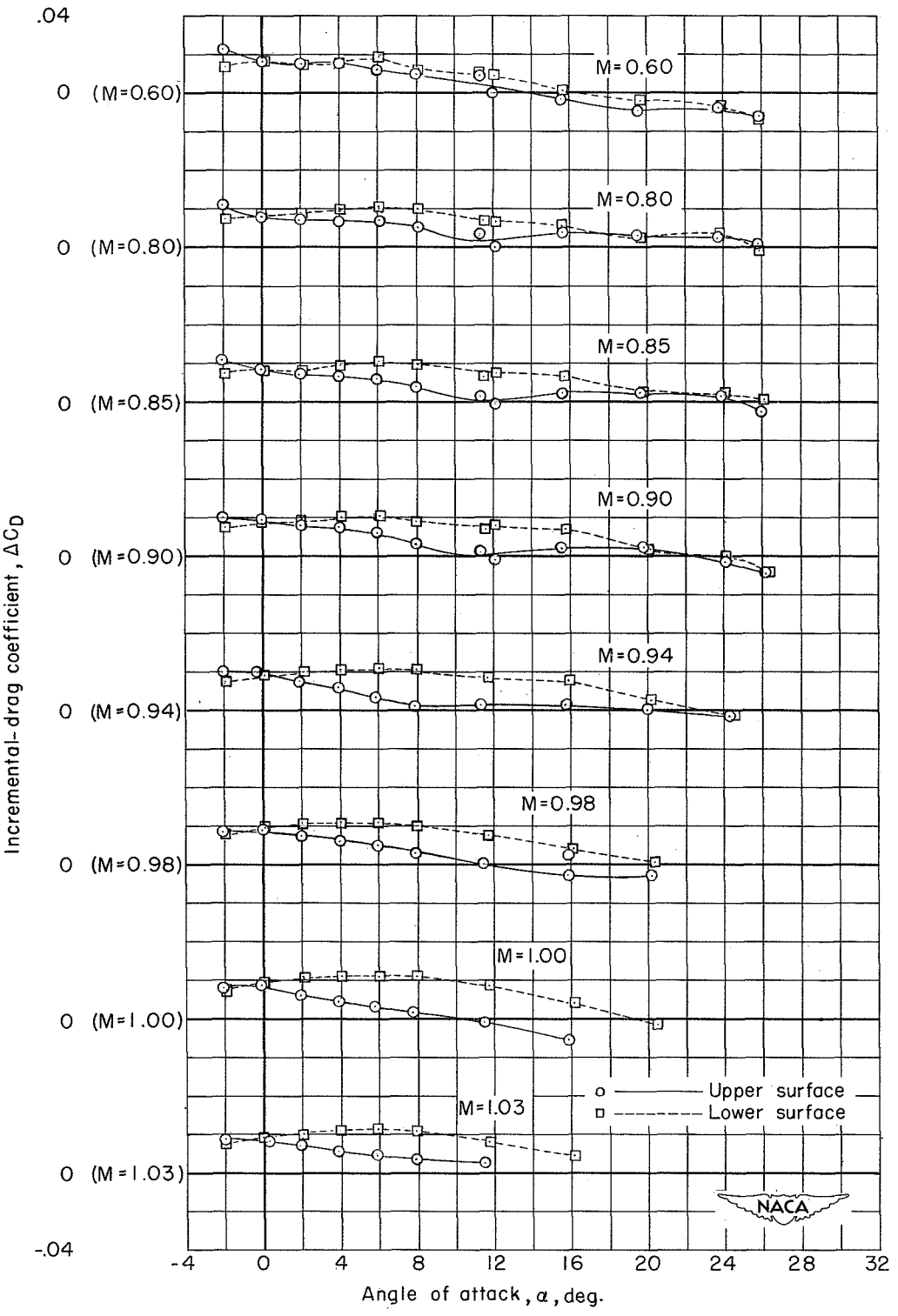

(e) Incremental-drag coefficient.

Figure 6.- Continued.

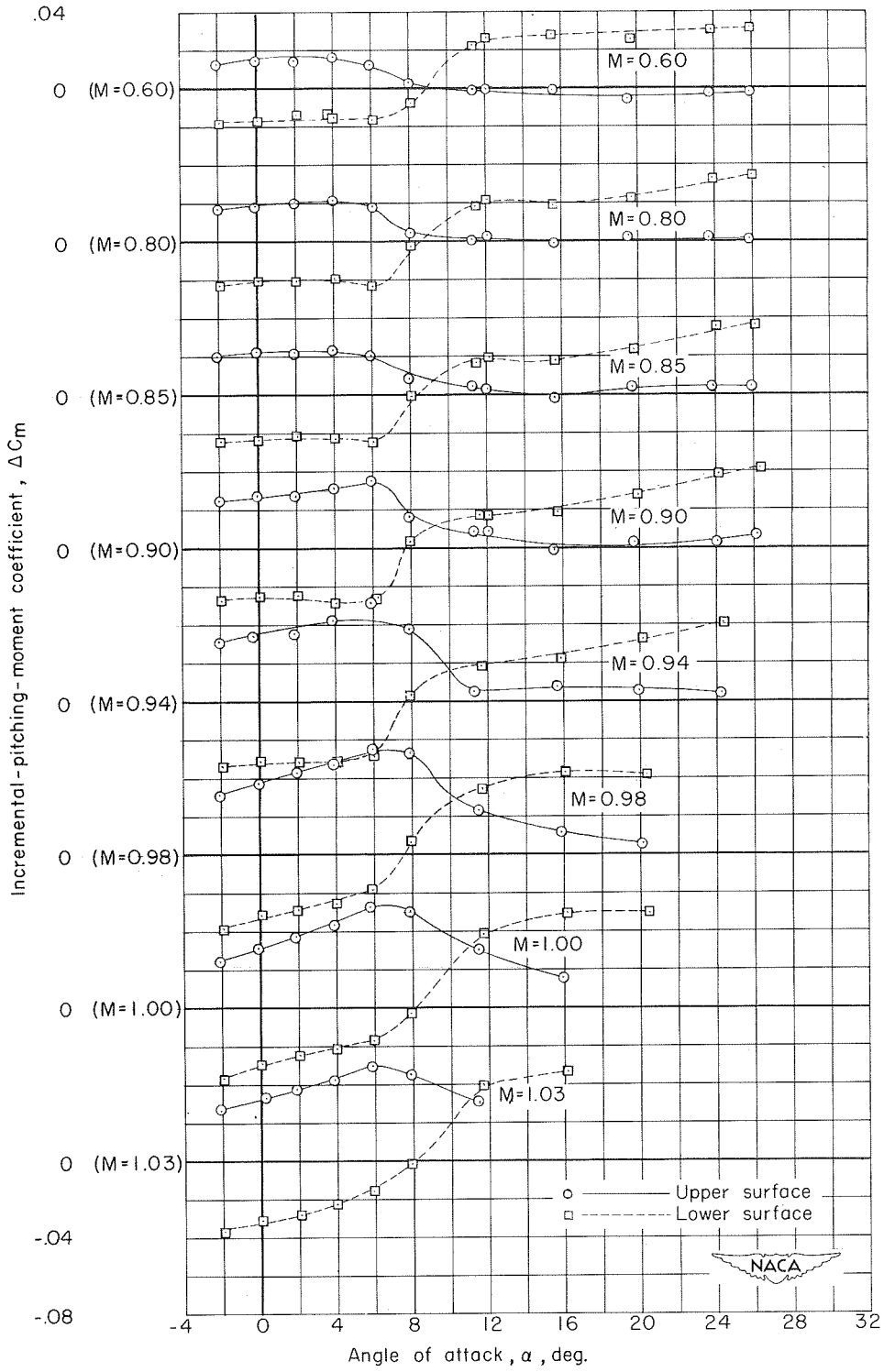

(f) Incremental-pitching-moment coefficient.

Figure 6.- Concluded.

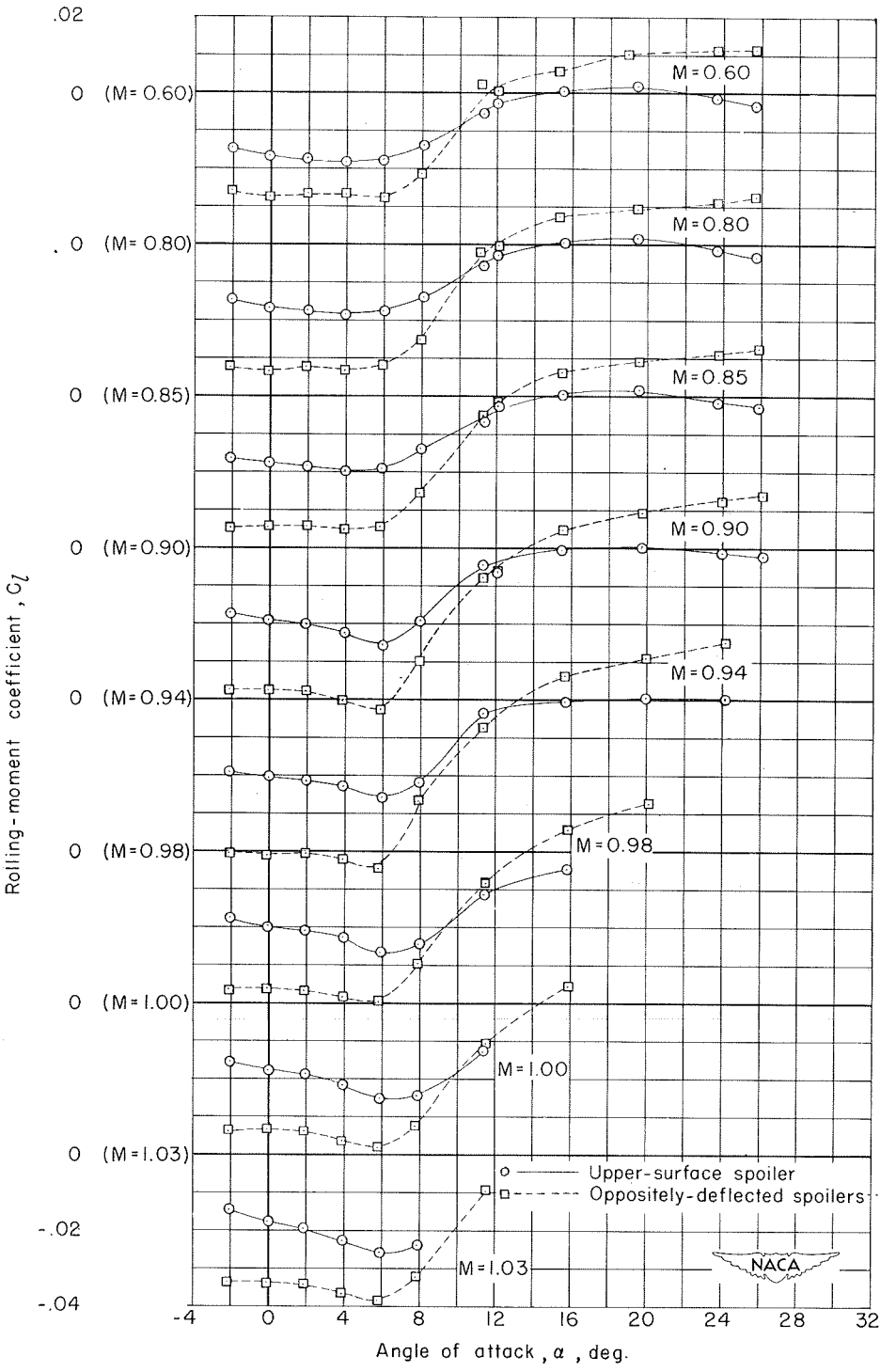

(a) Rolling-moment coefficient.

Figure 7.- Comparison of the aerodynamic characteristics of an upper-surface spoiler with oppositely deflected spoilers. No wing gap.

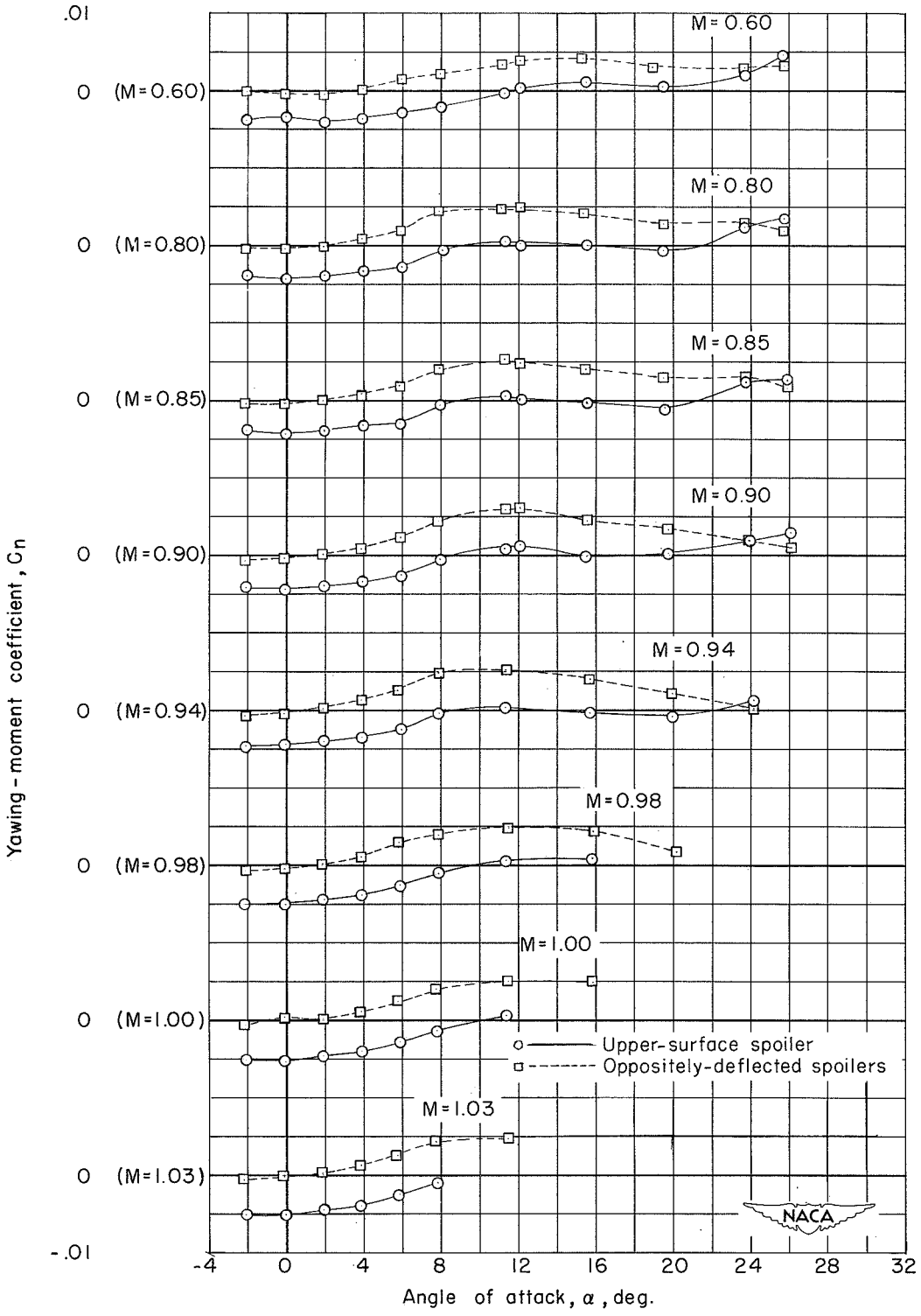

(b) Yawing-moment coefficient.

Figure 7.- Continued.

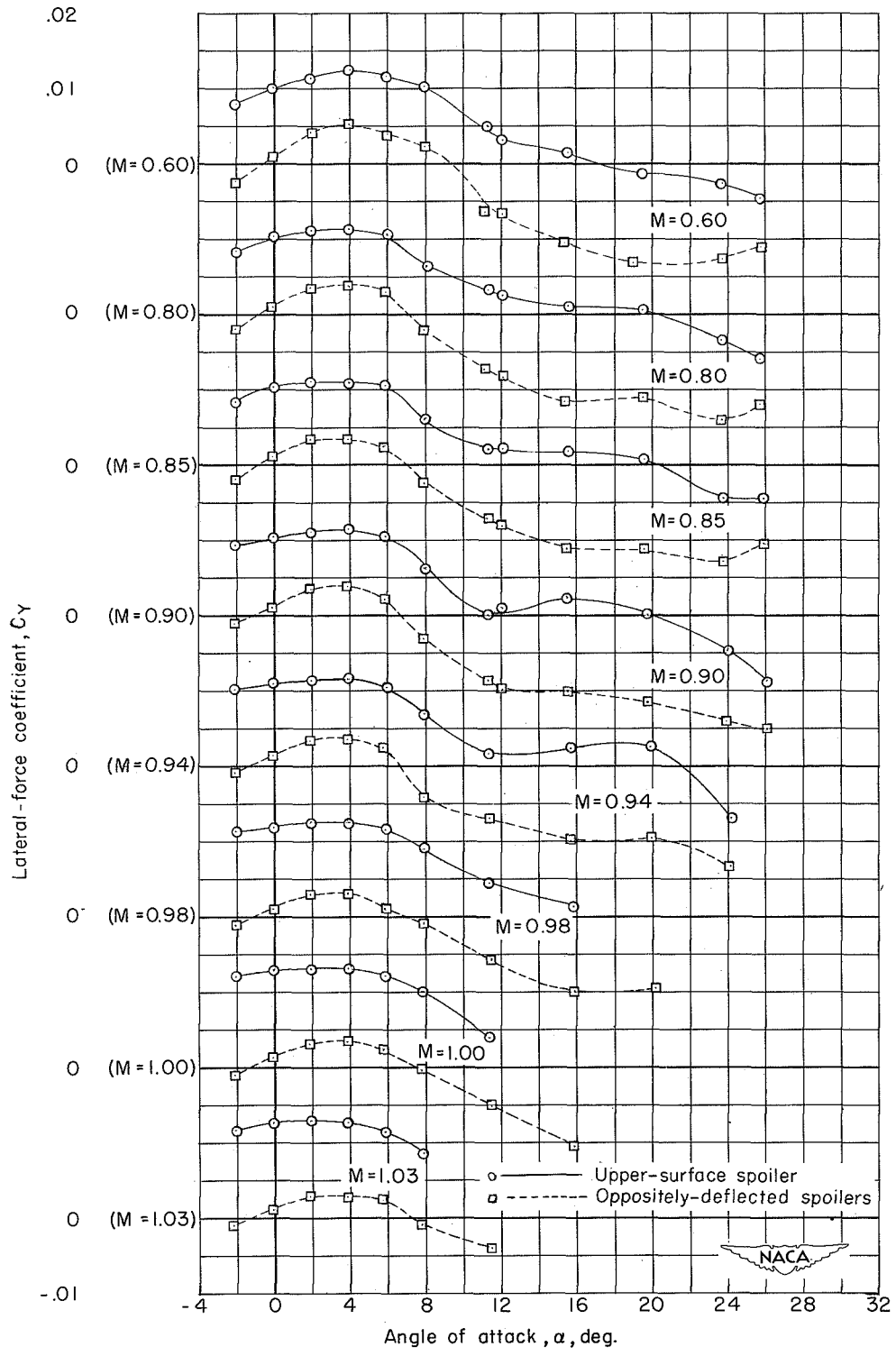

(c) Side-force coefficient.

Figure 7.- Continued.

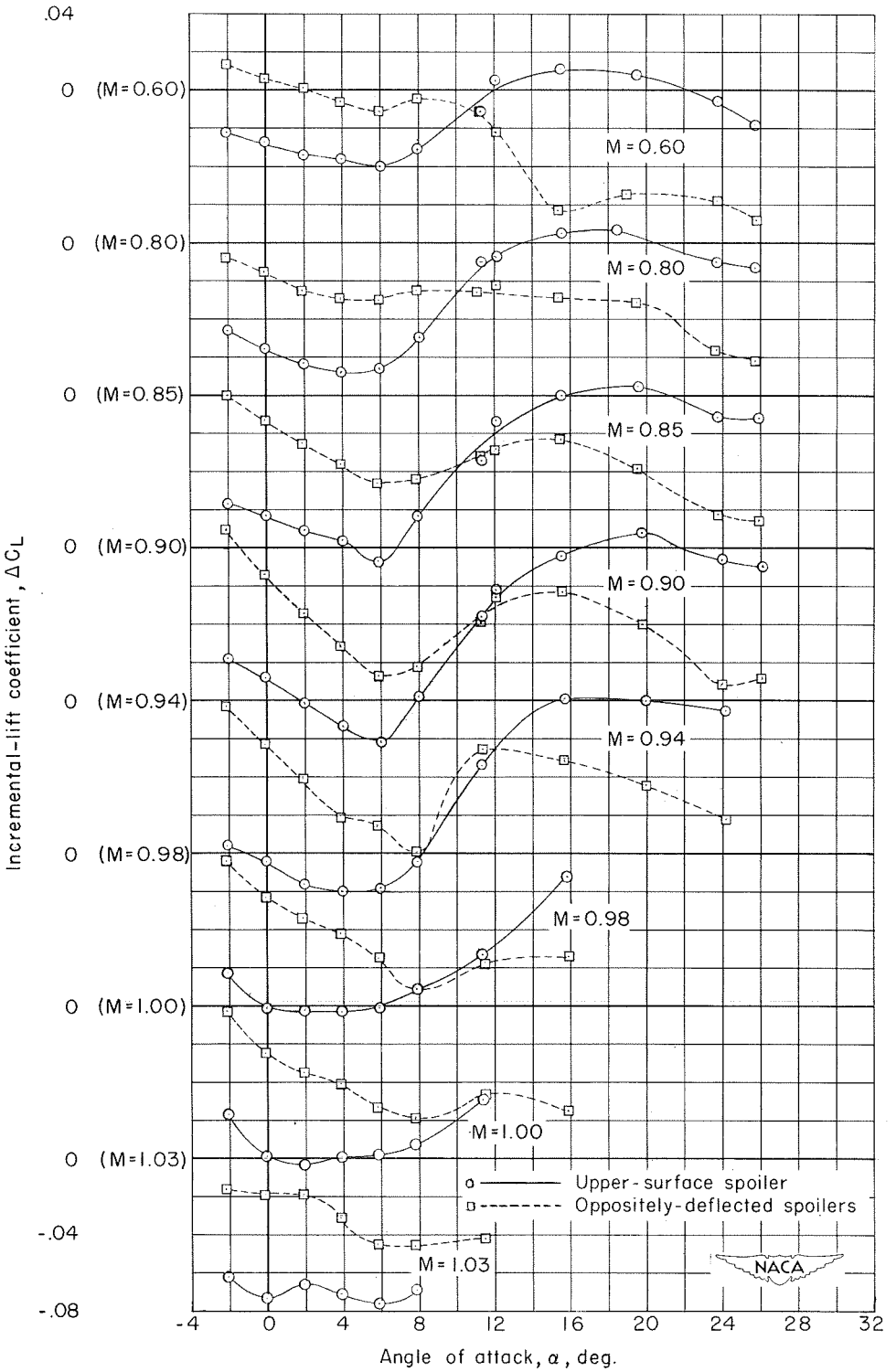

(d) Incremental-lift coefficient.

Figure 7.- Continued.

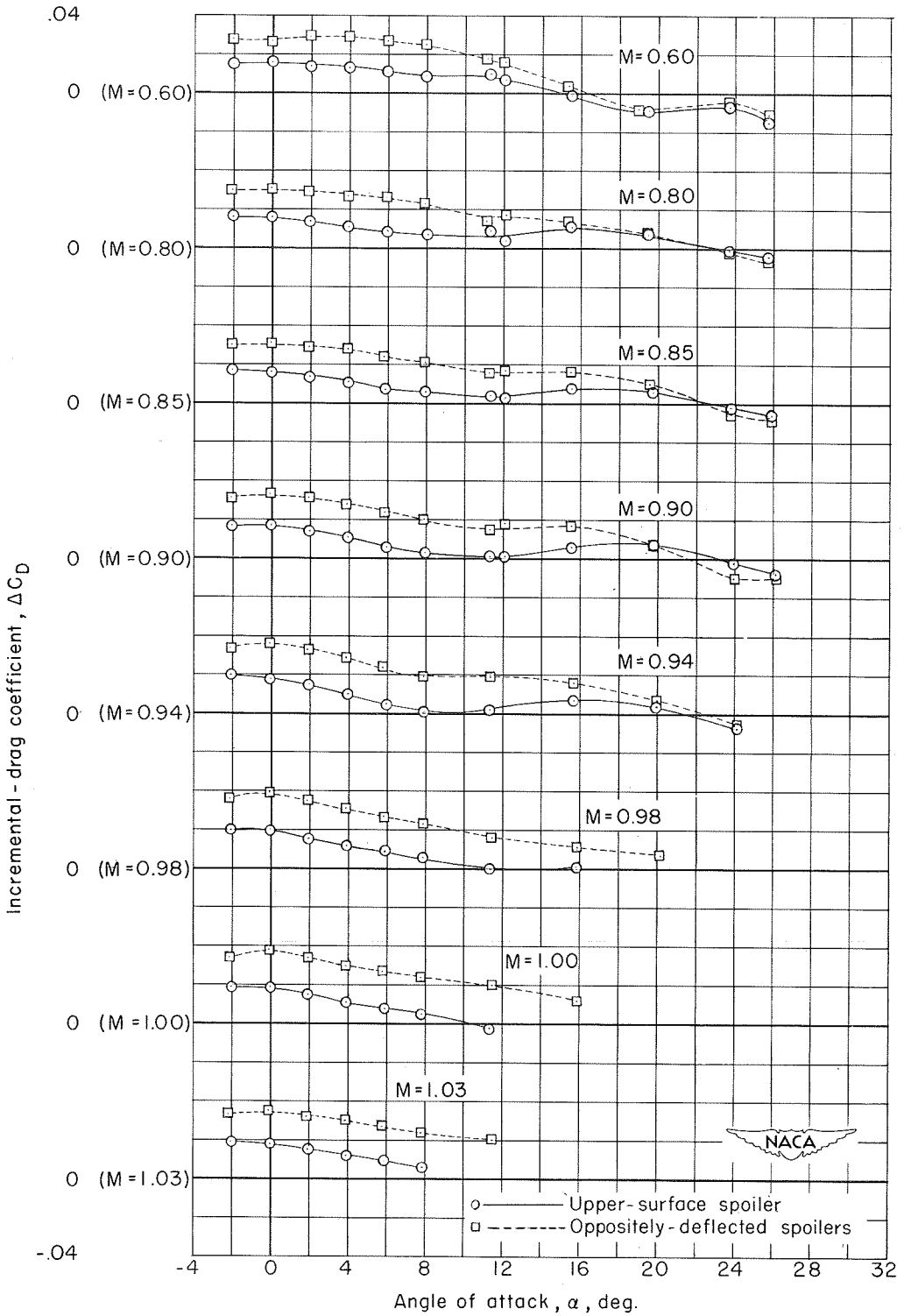

(e) Incremental-drag coefficient.

Figure 7.- Continued.

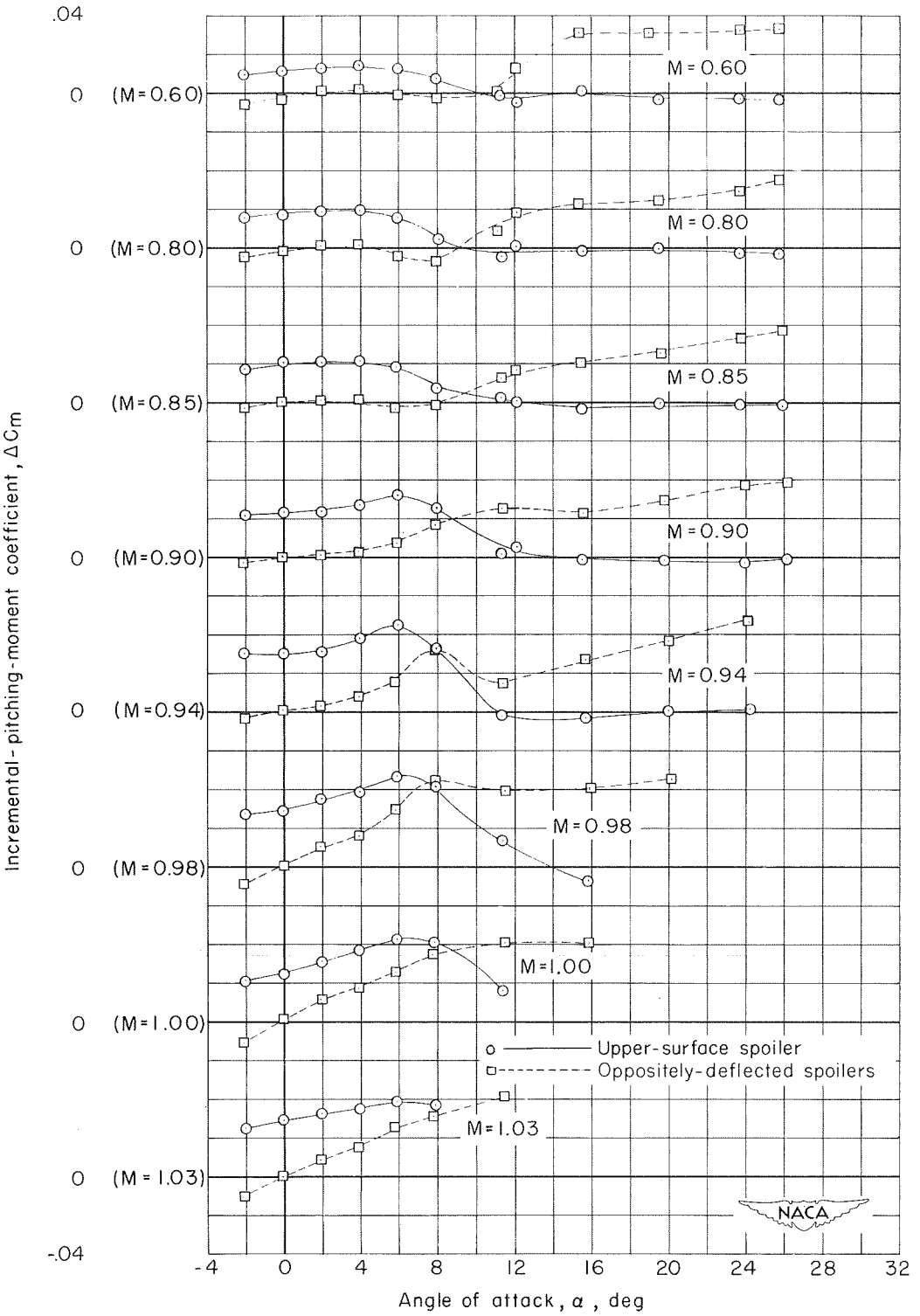

(f) Incremental-pitching-moment coefficient.

Figure 7.- Concluded.

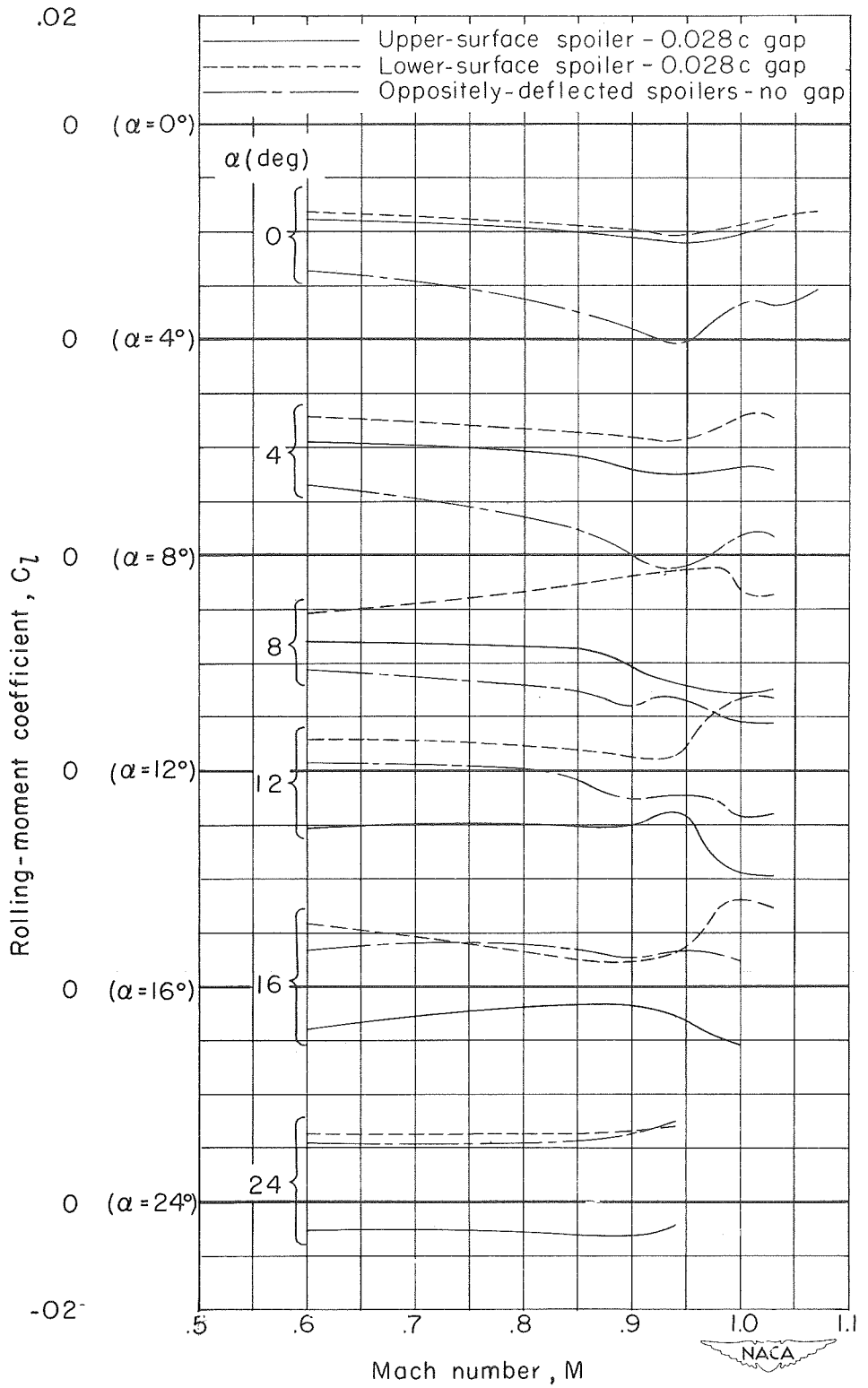

Figure 8.- Effect of Mach number on the rolling-moment coefficient of several spoiler configurations.

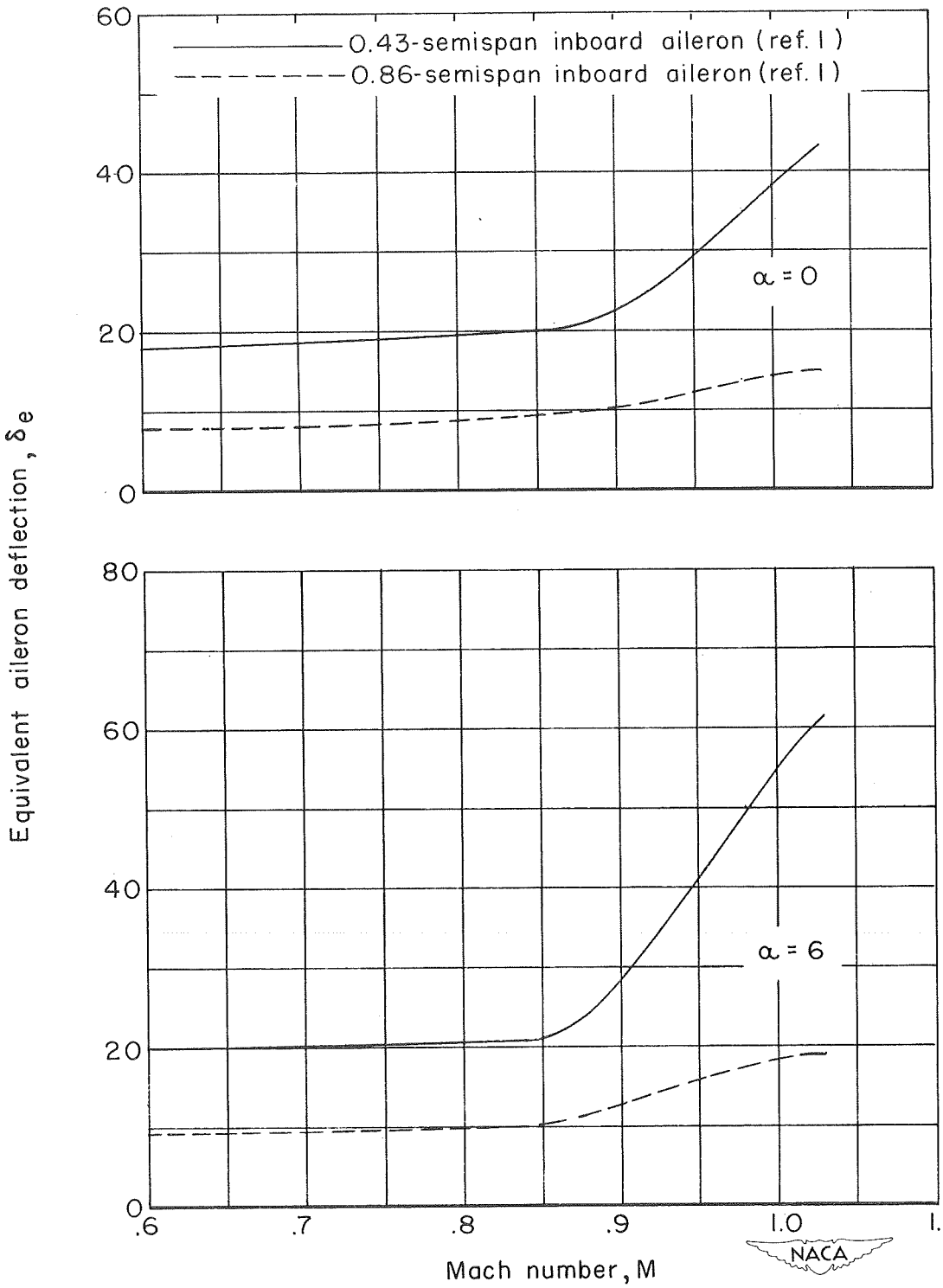

Figure 9.- Approximate deflection of a 30-percent-chord flap-type aileron required to produce the same rolling moment as the upper-surface spoiler with 0.028c wing gap. (Ref. 1)

Restriction/Classification
Cancelled

Restriction/Classification
Cancelled